A Novel Approach for Bi-directional Energy Metering Based on Integrated Rooftop SPV Systems

A dissertation submitted in fulfillment for award of degree

of

Master of Engineering

in

Power Systems

Submitted By

Harjeet Singh Bedi

(Roll No. : 801542006)

Under the Guidance of

Dr. Mukesh Singh

Associate Professor, EIED

&

Mr. Nirbhowjap Singh

Assistant Professor, EIED

Electrical & Instrumentation Engineering Department

Thapar University, Patiala

June 2017

Certificate

I hereby certify that the work which is being presented in this dissertation entitled ***A novel approach for bi-directional energy metering based on integrated rooftop SPV systems*** as a part of curriculum during Master of Engineering in Power Systems, submitted to Electrical & Instrumentation Engineering Department of Thapar University, Patiala, is an authentic record of my own work carried under the supervision of **Dr. Mukesh Singh and Mr. Nirbhowjap Singh**. It refers others researchers work which are duly listed in the reference section. The matter contained in this dissertation has not been submitted, neither in part nor in full to any other degree to any other university or institute except as reported in text and references.

Date: 31/July/17
Place: PATIALA

(HARJEET SINGH)

It is certified that the above statement made by my student is correct to the best of my knowledge and belief.

Dr. Mukesh Singh
Associate Professor
EIED, Thapar University

Mr. Nirbhowjap Singh
Assistant Professor
EIED, Thapar University

Acknowledgment

First and foremost I take the privilege to offer my deepest sense of gratitude to **Dr. Mukesh Singh, Associate Professor, EIED, Thapar University, Patiala and Mr. Nirbhowjap Singh, Assistant Professor, EIED, Thapar University, Patiala**, for their commendable support and constant motivation throughout this dissertation. With deep humility, I thank them for all the insightful conversations and their valuable comments. Their guidance has helped me improving my knowledge and perspective towards the work. I will always be indebted. It is my pleasant privilege to acknowledge my profound gratitude and indebtedness towards **Dr. Ravinder Agarwaal, HOD, EIED, Thapar University, Patiala** and our P.G. coordinator **Ms. Manbir Kaur, EIED, Thapar University, Patiala** as well as all the faculty members and staff of Electrical and Instrumentation Engineering Department (EIED), Thapar University, Patiala, who have bestowed their guidance at appropriate times without which it would have been very difficult to proceed with my work. In the last, I would like to express heartfelt gratitude to my parents and friends who have constantly helped me to keep my morale high throughout the research work.

Harjeet Singh Bedi
801542006

Contents

List of Figures

List of Tables

Abstract

The major challenge for any utility grid is to balance the generation and load demand. Though the efficiency of grid is improving, but variation in load demand is increasing consistently. However, the variation in load demand can be reduced by integration of distributive generation (DGs). DGs include penetration of renewable energy sources (RES) like wind, hydro and solar into smart grid (SG). In this regard, the proposed work implements net energy metering (NEM) with rooftop connected SPV (solar photo-voltaic) energy using a bi-directional energy meter. In addition to it, a novel hardware design of IEC61000 and RoHS compliant net energy meter based on STPM34 controller has also been proposed. This energy meter is capable of calculating the net energy usage from the utility grid. The detailed architecture of net energy meter has been discussed along with the results. The data from the net energy meter is monitored through graphical user interface setup in PC using UART based control.

Keywords: Advance metering infrastructure, distributed generation, bi-directional energy meters, load monitoring, net energy metering, renewable energy sources, STPM34, smart grid, solar photo-voltaic systems, UART.

Abbreviations

AMI	Advance Metering Infrastructure
ASSP	Application Specific Standard Product
CT	Current Transformer
DFE	Digital Front End
DG	Distributed Generation
DSM	Demand Side Management
FiT	Feed in Tariff
GTI	Grid Tie Inverter
LPF	Low Pass Filter
MDMS	Metering Data Management Systems
NEM	Net Energy Metering
NRES	Non-Renewable Energy Sources
OMS	Outage Management System
PQM	Power Quality Management
RES	Renewable Energy Sources
ROC	Rogowski Coil Integrator
SG	Smart Grid
SPV	Solar Photo Voltaic

List of Symbols

E_{in}	Imported Energy
E_{out}	Exported Energy
E_{net}	Net Energy
P	Active Power/ True Power
P_{act}	Measured Active Power
P_{rea}	Measured Reactive Power
P_{app}	Measured Apparent Power
Q	Reactive Power
S	Apparent Power
V_{G1}	Voltage at utility end
V_{G2}	Voltage at output of GTI
Z_L	Line Impedence
δ	Phase angle between V_{G2} and V_{G1}

Chapter 1

Introduction

1.1 Penetration of Renewable Energy Sources

Electric energy is considered to be an important commodity for development of any nation. With the economic development of the nation, the electric infrastructure is also becoming more complex. Due to increasing complexity, the power system network is often loaded near its operational limits to maintain power generation and demand balance [1] in real time. During the peak hours of the day, the electric grid faces a large variation in load demand. Due to huge extent of variation in load demand, the traditional grids face challenges in meeting the generation with existing load demand [2]. The failure to maintain real time balance between generation and load demand can drift grid frequency up or down from the nominal value of 50Hz. This sometimes lead to overdraw of power from the electric grid resulting into blackouts or plunge disturbances [3–5] affecting grid reliability. Hence, in order to achieve grid reliability, it has become a prime concern for any power utility to generate enough power in order to meet the load demand.

In order to maintain balance between generation and load demand, more power is needed to be fed into the power system. The traditional grids are mainly dependent on non-renewable sources of energy(NRES) like fossil fuels (coal, oil & gas). The NRES fuel reserves are limited and are likely to get exhausted in next few years. In addition to this, their extensive use has adverse effect on environment and cause greenhouse emissions. Hence, there is need to encourage the eco-friendly energy resources and balance the energy gap between generation and demand by incorporating renewable energy sources (RES) into traditional grid. Moreover, the technological innovation and environmental incentives are changing the face of electricity generation, distribution and transmission. Centralized generating facilities are giving way to smaller, more distributed generation (DGs), partially due

to the loss of traditional economics of scale. DGs such as micro turbines, photo-voltaic, fuel cells and wind energy conversion system have lower emissions and exhibits the potential to have lower cost negating traditional economies of scale. Smart grid (SG) have the capability to address these issues and improvise the functionality of the traditional grids in existing power system network.

SG has different attributes like Advance Metering Infrastructure (AMI), Outage Management System (OMS), Power Quality Management (PQM), Demand response, Renewable Integration/Micro-grid and Smart Home Energy Management. AMI upgrades the functionality of electric grid by incorporating bi-directional communications and power. It facilitates features like monitoring, protection and optimum utilization of interconnected appliances and hence contribute to sustainability and agility of the grid. However, the keystone of AMI is capability of the interacting with multiple entities (e.g. intelligent devices, controllers) using smart infrastructure [6]. The smart infrastructure includes monitoring and controlling the flow of electric energy by transmitting information to intelligent appliances [7].

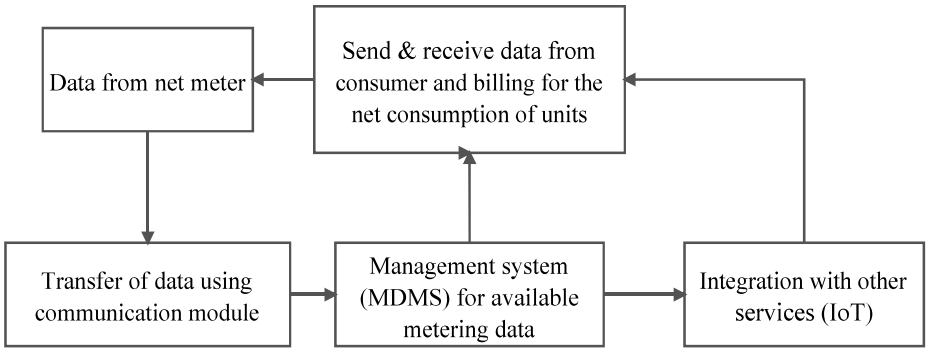

Figure 1.1: Advance metering infrastructure

Smart infrastructure includes the use of AMI, which allows bi-directional communication between the smart meter, consumer and utility grid [8]. It enables consumers to make intelligent decisions for monitoring and controlling energy consumption on the basis of information provided using bi-directional communication. In SGs, AMI is implemented with the use of smart meters, communication technologies and meter data management systems (MDMS) [9]. The improvised communication and metering technologies paved a way for incorporation of distributed generation (DGs) into the SG. DGs includes penetration of RES like solar, wind, hydrothermal and geothermal energy which creates an environment of interoperability, bi-directional communication and power flow.

1.2 Net Energy Metering

The penetration of RES in the electric grid has brought a drastic change in the power sector by evolving the consumers as producers of electric power [10]. Such type of consumers are called prosumers, which are capable of generating or procuring the load demand from RES generation installed at their premises [11, 12]. However, the RES are dependent on weather, time and large number of uncertainties. So, there may arise a case when power from RES may not be available to meet the load demand. Under such a condition, the load demand would be met through power imported from the grid.

Based on the above scenario, a scheme known as net energy metering (NEM) using rooftop solar photo-volatic (SPV) technology has been presented in this thesis. Solar energy is extracted using solar photo-volatic panels in the form of DC power. This DC power is fed into grid tied inverter (GTI) for conversion of DC power into AC power. The GTI also synchronizes the solar power with the utility power by matching the voltage, phase and frequency between them.

The entire consumer's load is fed by power available through SPV and the utility power such that generation must meet the load demand in all conditions. During anytime in a day, when excess power generated via SPV generation is available at consumer's end, it can be offset back to grid [13, 14]. In other words, NEM can be defined as the metering of net units consumed by the consumer by offsetting some or whole of excess power generated through renewable sources installed at its premises. However, in absence of SPV energy, the power would be imported from the grid to meet load demand. The metering of this bi-directional exchange of power has been a challenging task. Logically, when power is being imported from the grid, the energy meter would move forward; and it moves backwards when power is being exported from the grid [15]. Hence, to measure this two way exchange of power, a bi-directional energy meter [16] is proposed in this dissertation. It is capable of measuring two way flow of energy through the line and calculates the net units consumed by the consumer. The Fig. 1.2 shows the schematic diagram of NEM system.

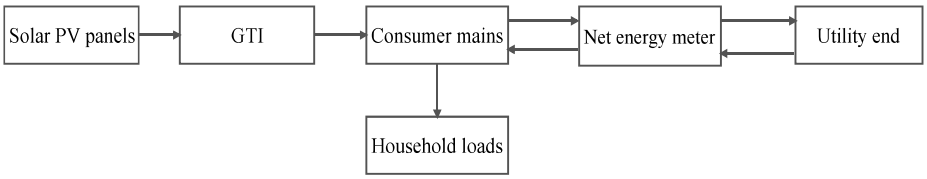

Figure 1.2: Schematic of NEM system

1.3 Literature Review

Smart grids are next generation grids aimed to achieve the minimization of gap between electricity demand and generation with scope of integration of renewable energy sources such as solar photo-volatic systems [17]. The use of renewable energy sources (RES) promote the green energy and also reduces the transmission and distribution losses (T & D losses) [18]. Furthermore, the RES enables reduced congestion on distribution network, minimized generation cost with stabilized frequency and voltage. One of the popular applications of smart grid is to evolve consumers as prosumers (producers as well as consumers) of electricity at distribution end [19]. Net energy metering (NEM) is a mechanism which allows prosumers to offset some or whole of the electric energy generated using solar photo-voltaic (SPV) systems installed at their premises [20]. In return, the prosumers gets advantage in the form of incentives or reduced bill costs annually. Also, it encourages the consumer towards the energy savings by shifting their peak load consumption from the utility supply to renewable generation.

Mostly, the previous works on net metering were based on the economic aspects of net metering scheme. In [21], an economical comparison between NEM and FiT tariffs with application of incentive policies in the micro-grid has been discussed. The net metering proved to have significant savings on bill as compared to feed in tariff systems as well as conventional metering systems [22]. In other aspect, in [23], a scheme was proposed to store excess energy generated from rooftop SPV system when price of exporting energy is low. Unfortunately, the higher cost of batteries acts as a limitation of the work and discourages domestic consumers to invest in RES systems. Hence, net metering system without batteries should be preferred.

The metering of net energy requires the use of a meter which is capable of measuring energy flowing bi-directionally on the line. In general, two unidirectional meters are used to measure the import and export on the line. However, the it adds additional cost on the consumer's pocket. This additional cost can be reduced with the use of net energy meter. The net meter records the consumption of energy from utility while recording the excess energy, generated through SPV systems, sent back to utility after self-consumption. A GSM/GPRS based smart home controller with the use of net energy meter proposed in [24] was based on LPC2148 processor. GSM/GPRS based technology suffers from disadvantages such as poor reliability and incurred charges on consumer for usage. In this context, a hardware design of a net energy meter was proposed in [25], based on LonWorks technology which uses echelon neuron processor. However, the work was solely based on remote monitoring and it lacked control techniques for demand side management (DSM).

Further, ATmega 328 based net energy meter has been suggested in [26] to measure export and import of energy. The lack of control and monitoring strategies using energy meter highlights the limitation of the proposed work.

Thus, to overcome the above outlined challenges, the work proposed in this dissertation is based on net energy metering using a net meter. The dissertation consists of basic knowledge of net energy metering along with detailed architecture. In addition to it, a novel hardware design of IEC62053 and ANSI 12.2 standard net meter using STPM34 based controller is presented. STPM34 is application specific standard product (ASSP) dedicated energy metering chip embedded on EVALSTPM34 development board. It consists of 2^{nd} order 24-bit ADC which can provide more accuracy in measurement than any other energy meters. The additional features constitute the overcurrent protection and monitoring, under and overvoltage detection, monitoring and dual mode apparent energy calculation.

1.4 Research Gap

The energy gap between generation and load demand has to be filled with the penetration of RES in smart grid. This dissertation discusses the net energy metering enabling the penetration of renewable energy sources such as rooftop connected SPV systems. The excess energy available from the grid can be stored in batteries or can be sold to the utility when price of exporting is high [23]. Unfortunately, the high market costs of batteries increases the capital cost of the system. Since, NEM is based on two way exchange of power, the net units are measured by a net meter. In this regard, a net meter with smart home controller based on GSM/GPRS technology using LP2148 controller was proposed in [24]. The GSM/GPRS based metering is unreliable and required fixed GSM number to communicate. Another hardware design of net meter is based on two ATT7022 controllers was implemented to realist the concept of net metering [27]. However, the communication module was not discussed in the paper which limits the scope of two way communication feature of smart grid. The outlined work in previous researches also lacked calibration module in order to enhance the accuracy of metering parameters.

To address these issues, the work proposed in this dissertation is based on NEM to balance load demand and generation. In the proposed work, rather than storing energy in battery, it is being stored on the grid. In addition to this, a novel design of net energy meter based on dedicated energy metering ic STPM34 is proposed to measure the net units consumed by the consumer from the grid. The metering parameters are calibrated so that very high precision can be obtained while measuring.

1.5 Motivation and Objectives

The traditional grids face challenge in maintaining balance between electricity generation and consumption. The problem becomes adverse during peak load hours and thus causes the power system network to be overstressed. This leads to various problems like power outages, frequency variations and rapid blackouts. This issue is well addressed with penetration of renewable energy sources in the smart grid. In this context, net energy metering offers a platform to encourage the consumers to use renewable energy sources such as solar photo-voltaic (SPV) systems. The consumer's load is entitled to be fed through SPV systems and excess energy is sent back to distribution network. The utility supply can be used as backup when energy from SPV system is not available. The net exchange of energy between utility and consumer is measured using net meter. It is observed that the net energy metering is an economical and effective technique to reduce burden on the power system network during normal as well as peak hours of the day.

1.5.1 Objectives

The major contributions of this dissertation is summarized as follows:-

- To implement net energy metering system for rooftop connected SPV system without using battery as energy storage.
- To implement a novel hardware design of IEC61000 and RoHS complaint net energy meter based on STPM34 controller to measure voltage, current and net active, reactive and apparent power flow on the line.
- To observe the value of imported energy, exported energy and net energy consumed from the net meter .
- The data from the net energy meter is monitored using graphical user interface using UART based data interface. This data can be useful resource for utility to determine energy forecasting, peak time shaving and time of use pricing.

1.6 Organization of the dissertation work

- **Chapter 1:** This chapter includes the brief introduction about the net metering system. Based on it, a literature survey has been performed to get a detailed analysis of various aspects of net metering. Then, research motivation in the field of net metering has been described. In the end, objectives for dissertation work is formulated.

- **Chapter 2:** The system description of net metering using SPV system is explained in addition to proposed system. The net metering concept is explained in detail with the help of equations and figures. The proposed design of net energy metering system has also been discussed.

- **Chapter 3:** The architecture of net energy meter is presented in this section. This chapter include brief discussion about the analog and digital module of the net energy meter along with power supply and microcontroller STPM34.

- **Chapter 4:** This chapter contain the different algorithms designed for calculating different parameters of electricity such as voltage, current, frequency, power factor, active, reactive and apparent power and imported energy, exported energy and net energy.

- **Chapter 5:** Results obtained from net energy meter are plotted against the measured values and briefly discussed.

- **Chapter 6:** In the end, conclusion has been briefed with future scope of the presented work.

Chapter 2

Net Metering System Description

This dissertation implements the concept of net energy metering (NEM) on smart home integrated with rooftop SPV system. The consumer is expected to fulfill the its entire load from the power available through SPV systems. Through NEM, the SPV owner connects its system with the main grid and feeds excess power generated in to distribution system. The utility companies, as per state policies, would provide incentives for the excess power fed to the grid. However, when the SPV generation is not sufficient enough to meet the loads, the utility company would supply electrical needs. Hence, the consumer is charged on the basis of net units ($P_{G1(NET)}$) supplied by the utility.

In simple terminology, NEM can be understood as a meter which spins forwards when energy is taken from the utility and spin backwards when energy is sent to the grid. Hence, the net units are calculated. The billing credits are given on those net units. NEM allows the consumer to store excess energy on the grid instead of storing in large batteries. Thus, it reduces the cost of storing energy. Also, the energy can be used again by the consumer whenever it is needed. Moreover, the utility buys energy at very good price in case of peak demand thus causing technical and economic benefit to both. The use of NM with SG can result in great saving of energy and money. Also, it can help in improving the power quality which is frequent demand by the consumers.

The additional advantage of NEM is that it allows the consumer to store excess energy on the grid instead of storing in large batteries. Thus, it reduces the cost of storing energy and use of batteries to store excess energy is eliminated. This results in reduction of overall cost of the system due to elimination of high cost batteries. Also, the energy can be used again by the consumer whenever it is needed. In this way, this system allows consumers to produce hassle free power with almost negligible maintenance costs. The single line diagram of net metering is shown in Fig. 2.1. As per given diagram, generation is expected

to satisfy the load demand at any time interval of the day. However, due to intermittent nature of SPV, two scenarios are expected:

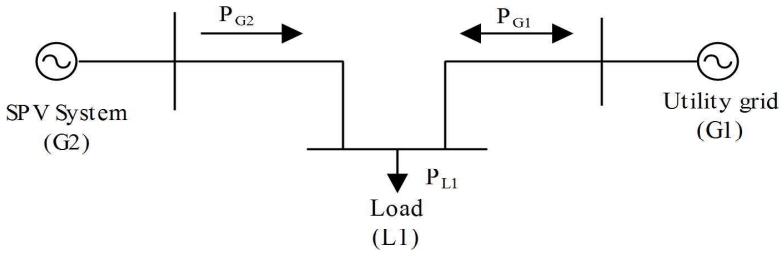

Figure 2.1: Single line diagram of flow of power in NEM

Scenario- I

When power from SPV may not be available to feed the load demand. In such a scenario, some power may need to be imported from the grid to meet the load demand.

Scenario- II

When sun is at its peak and ample energy is available at consumer's end. In such a scenario, excess power instead of storing can be sent back to the grid.

During these scenarios, the small interruptions of power goes unnoticed due to instantaneous switching between utility grid and SPV systems. This results in smooth power reversals on the line causing minimal inconvenience to the consumer. The block diagram in Fig. 2.2 represents the working of NEM system. As depicted in this figure, the NEM system consists of three components: utlity grid supply (P_{G1}), SPV generation (P_{G2}) & consumer's load (P_{L1}). The output of SPV system (DC power) is connected to grid tie inverter (GTI) for conversion of DC to AC as well as synchronizing the SPV power with the grid.

To ensure proper synchronization of SPV power with the grid, a GTI must follow two conditions. Firstly, the output voltage and phase must match with grid. Secondly, the frequency of the output power from GTI must be same as that of the grid [28]. The real and reactive power injected by GTI into the utility grid is given as:

$$P = \frac{|V_{G2}||V_{G1}| * sin\delta}{Z_L} \tag{2.1}$$

$$Q = \frac{|V_{G2}|^2}{Z_L} - \frac{|V_{G2}||V_{G1}| * cos\delta}{Z_L} \tag{2.2}$$

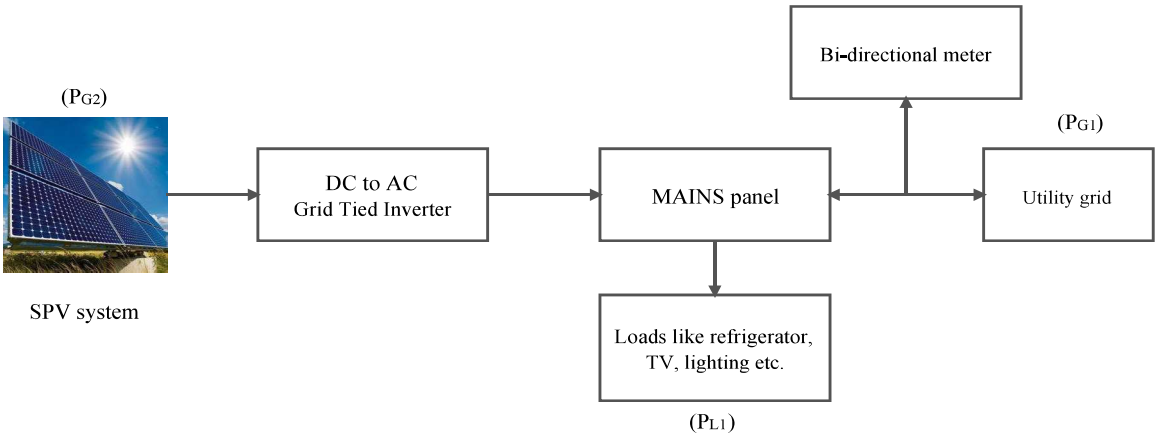

Figure 2.2: Block diagram of NEM

where, V_{G2} is the output voltage of grid tied inverter (GTI), V_{G1} is the utility side voltage, Z_L is line impedance and δ is the phase angle between V_{G2} & V_{G1}.

In grid tied inverters, PLL synchronization techniques are widely used due to fast response to grid synchronization, frequency variation and extent upto which it can remain synchronized inspite of poor quality voltage. The PLL synchronization technique estimates the phase angle of the utility grid voltage V_{G1}. Then, after generating a quadrature voltage vector($V_{\alpha\beta}$) in stationary frame, it is transformed into synchronous frame vector (V_{dq}). Further, with the use of a PI controller the voltage (V_q) is regulated to zero and phase angle is extracted [29]. In addition to this, using phase angle detection, GTI also detects the islanding conditions (such as grid failure, power outage) in a grid and provides safety of personnel and equipments [30]. The output power from GTI is connected through mains panel with the utility and consumer loads.

2.1 Proposed system

The proposed system for net energy metering is shown in Fig. 2.3. In this system, when $P_{G2} < P_{L1}$, deficit power is obtained from grid through the same power line.

Thus, the import of power from grid to consumer will be as shown:

$$P_{G1(Import)} = P_{G2} - P_{L1} > 0 \tag{2.3}$$

where, $P_{G1(Import)}$ is the power imported from grid

When $P_{G2} > P_{L1}$, excess power will be sent back to grid through the same power line. The export of power from consumer to grid will be as shown:

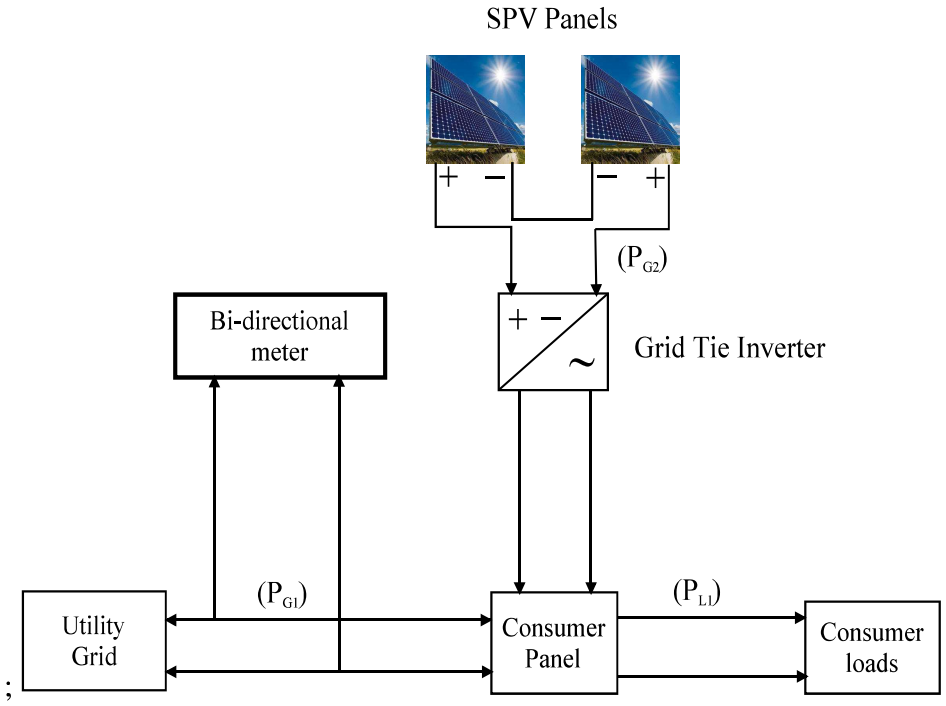

Figure 2.3: Proposed design of NEM system

$$P_{G1(Export)} = -(P_{G2} - P_{L1}) < 0 \tag{2.4}$$

where, $P_{G1(Export)}$ is the power injected into grid

The negative sign indicates the excess power being injected into the grid. Hence, the consumer is billed only the net units supplied from utility company. The net units ($P_{G1(NET)}$) is calculated as shown below:

$$P_{G1(NET)} = P_{G1(Import)} - P_{G1(Export)} \tag{2.5}$$

where, $P_{G1(NET)}$ is the net power supplied by the grid

However, to measure these net units, a bi-directional energy meter is required. Hence, a hardware design of bi-directional meter has been proposed in next section to measure the net units of P_{G1} consumed as well as SPV generation (P_{G2}) at consumer's end.

Chapter 3

Architecture of Net Energy Meter

The net units consumed by consumer are measured with the help of a bi-directional energy meter. This paper presents the hardware design of a single phase bi-directional energy meter based on STPM34 controller. The STPM34 is an application specific standard product (ASSP) used specifically for metering applications. The block diagram of single phase bi-directional energy meter based on STPM34 controller is shown Fig. 3.1. The STPM34 controller consists of an analog and digital module.

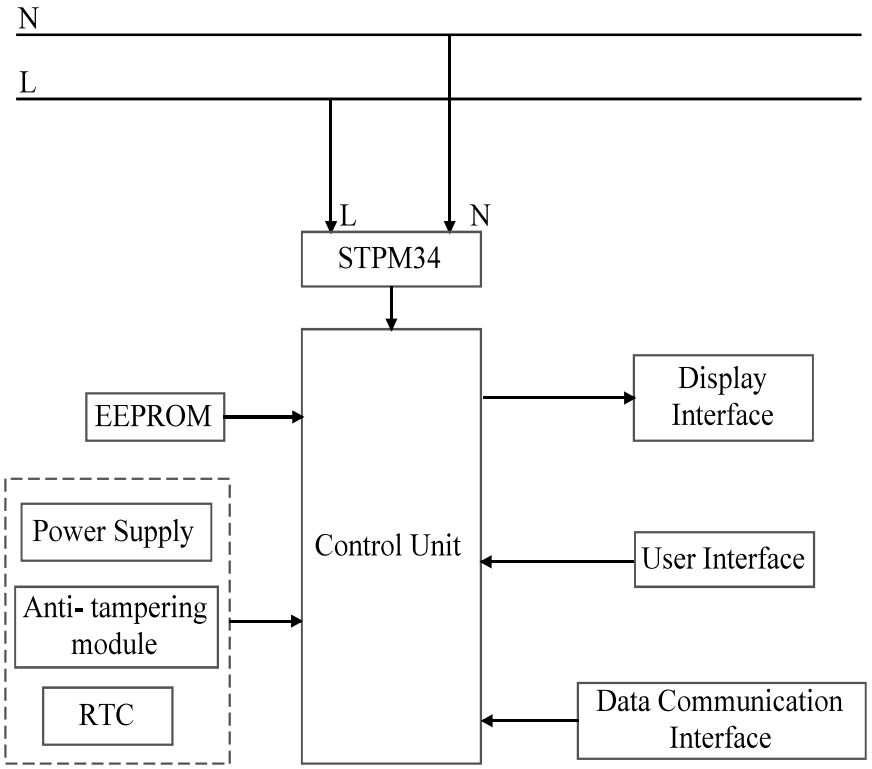

Figure 3.1: Block diagram of bi-directional energy meter

The analog module includes low offset amplifiers, 24-bit ADCs and two voltage references. The digital module includes filtering section, hardwired DSP and serial communication interface (SPI or UART). The proposed energy meter is capable of performing four quadrant operation and provides accuracy of class 0.2. The pin diagram of STPM34 is shown in Fig. 3.2.

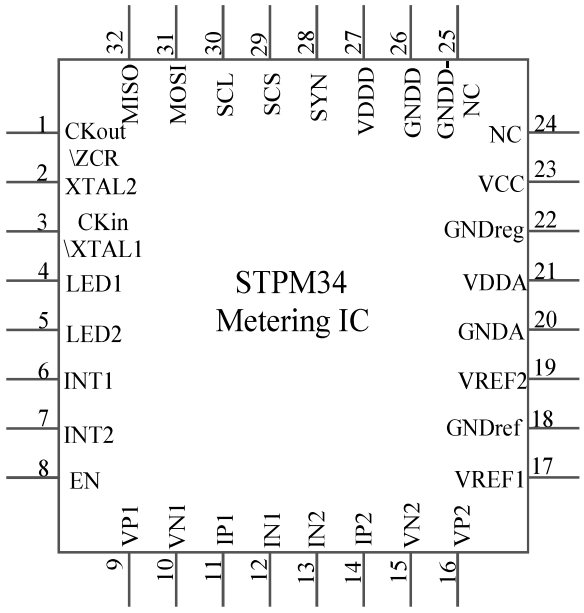

Figure 3.2: Schematic of STPM34

The use of STPM34 in energy metering is more advantageous than other controllers such as arduino and peripheral interface controllers (PIC). These controllers are open source based controllers and are meant to be used in variety of applications. However, STPM34 is designed specifically for energy metering purposes and programmed for operations related to metering of energy only. This results in reduction in the length of the program, unlike programming in PIC. Moreover, the STPM34 consists of 2^{nd} order 24-bit ADC as compared to 10-bit ADC used in MSP430 energy metering chip of texas instruments. Hence, degree of precision is more and better precision in measurement is achieved. In addition, it is capable performing dual mode energy operation with relatively high processing speed. Due to these outlined features, the STPM34 is preferred over the other controllers.

The architecture of STPM34 based net energy meter consists of analog and digital modules [31].

3.1 Analog module

The analog module consists of fully differential voltage and current sensing circuits.

3.1.1 Voltage Sensing Circuit

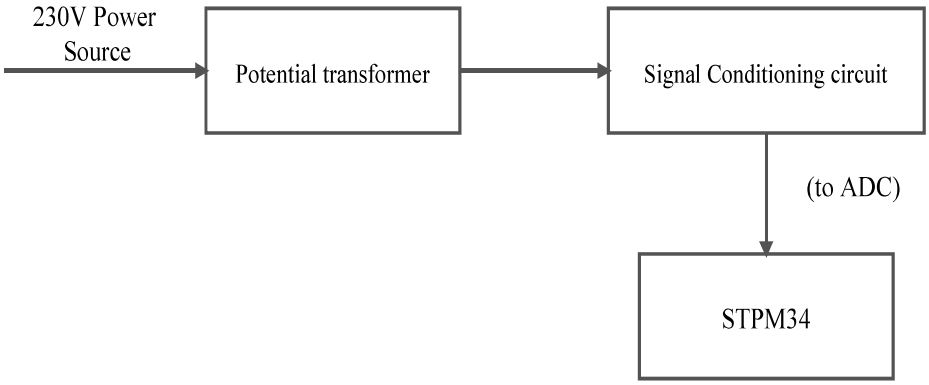

Figure 3.3: Block diagram of voltage sensing circuit

The block diagram of voltage sensing circuit is shown in Fig. 3.3. In voltage sensing circuit, the high voltage input is stepped down to a voltage level, in order to be interfaced with the microcontroller unit. This circuit consists of a potential divider, a signal conditioning circuit and ADC (in-built with STPM34). The initial supply voltage signal is scaled down to a lower value using a potential divider. Further, the reduced voltage signal is fed to signal conditioning circuit for filtering and is made input at pin 9 of STPM34. Finally, the filtered signal is send to the second order 24-bit ADC of STPM34 so that analog signals can be converted into digital signals.

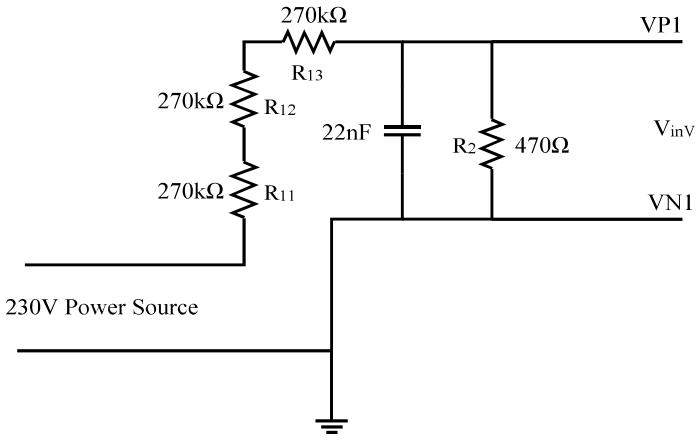

Figure 3.4: Voltage sensing circuit

The schematic of voltage sensing circuit is shown in Fig. 3.4. The scaled down voltage input (V_{inV}) at the input channel of STPM34 is calculated as:

$$V_{inV} = \frac{R_2}{R_{11} + R_{12} + R_{13} + R_2} * V_{line} \tag{3.1}$$

where, R_{11}, R_{12}, R_{13} and R_2 are the voltage divider resisters.

Further, this voltage is fed into the in-built 24-bit ADC for conversion of analog signal into binary sigma-delta signal. The resulting voltage after conversion by ADC is given as:

$$V_{\Delta\Sigma} = V_{inV} * \frac{A_V}{V_{ref}} \tag{3.2}$$

where, $V_{\Delta\Sigma}$ is the converted binary signal, A_V is the pre-amplification gain of value 2 and V_{ref} is the reference voltage set at 1.18V.

The RMS value of the voltage is calculated at an interval of 128μs and is given as:

$$V_{RMS} = Dec_v * \frac{V_{ref} * (1 + \frac{R_1}{R_2})}{cal_v * A_v * 2^{15}}[V] \tag{3.3}$$

where, Dec_v is decimal value of measured RMS voltage, V_{ref} is voltage reference of 1.18V, resistors R_1(= R_{11}+R_{12}+R_{13}) & R_2 are voltage divider resistors, cal_v = 0.875 and A_v is voltage gain of 2. The maximum RMS voltage which can be safely measured is given by:

$$V_{RMSmax} = \frac{1}{2} * \frac{V_{ref}}{A_v * \sqrt{2}} * \frac{R_1 + R_2}{R_2}[V] \tag{3.4}$$

where, V_{RMSmax} is the maximum RMS of measured voltage. The peak to peak voltage for given RMS value is given as:

$$V_{pp} = V_{RMS} * 2\sqrt{2}[V] \tag{3.5}$$

where, V_{pp} is the peak to peak voltage.

3.1.2 Current Sensing Circuit

The block diagram of current sensing circuit is shown in Fig. 3.5. The current flowing in the line is scaled down using current transformers (CTs). The current sensing circuit consists of CTs, signal conditioning circuit (anti-aliasing filter) and in-built 24-bit ADC. The input current is then made to pass through anti-aliasing RC filter to convert the reduced current signal in to suitable voltage signals to be input at pin 11 of the STPM34. Finally, the filtered signals feed 24-bit ADC for conversion of analog signals into binary sigma delta signals.

The schematic of current sensing circuit is shown in Fig. 3.6. The scaled down current is converted to proportional voltage signal (V_{inC}) and is available at input channel IP1 of STPM34 as:

$$V_{inC} = \frac{R_4}{2500} * I[V] \tag{3.6}$$

where, R_4 is known as burden resistor which convert current signal into proportional voltage

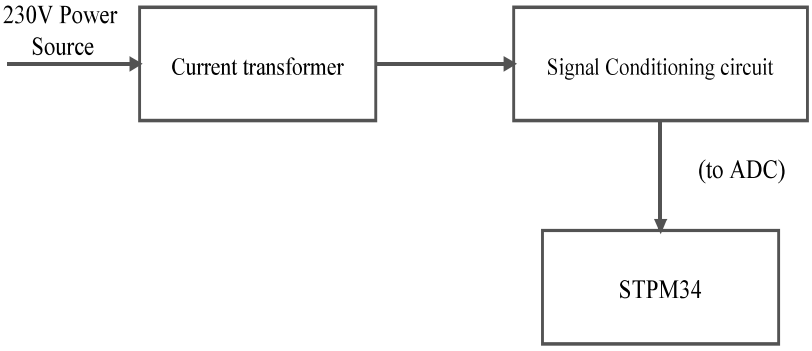

Figure 3.5: Block diagram of current sensing circuit

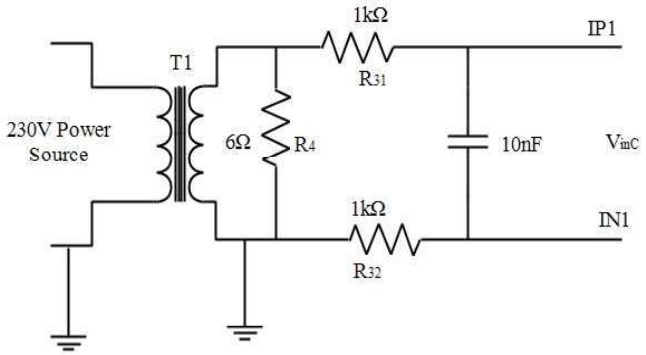

Figure 3.6: Current sensing circuit

signal & N is the turn ration of CT 1:2500.

This voltage signal is further fed into the in-built 24-bit ADC for conversion of analog signal into 2^{nd} order binary sigma-delta signal. The resulting signal is given after conversion by ADC is given as:

$$V_{\Delta\Sigma} = V_{inC} * \frac{A_i}{V_{ref}} \tag{3.7}$$

where, $V_{\Delta\Sigma}$ is the converted current binary signal, A_i is the pre-amplification gain of value 16 and V_{ref} is the reference voltage set at 1.18V.

The RMS value of current is calculated at an interval of 128μs and is given as:

$$I_{RMS} = Dec_i * \frac{V_{ref}}{cal_i * A_i * 2^{17} * k_{sen} * k_{in}}[A] \tag{3.8}$$

where, Dec_i is the decimal value of measured RMS value of the current, V_{ref} is the reference voltage set at 1.18V, cal_i & A_i are the calibration and pre-amplification gain set at 0.875 and 16 respectively and k_{sen} is current transformer sensitivity factor of 2.4mV/A.

The current transformer sensitivity (k_{sen}) can be calculated as:

$$k_{sen} = \frac{V_{ref}^2 * C_{pulses} * (1 + \frac{R_1}{R_2})}{1800 * A_v * Ai * cal_v * cal_i * Dclk} [mV/A] \tag{3.9}$$

Finally, the after processing of signals in analog front end, the voltage and current signals further feed digital front end for DSP, filtering and decimation processes.

3.2 Digital module

The signals after being processed through analog module are fed into digital module. Each voltage and current signal is processed through independent DSP which consists of DFE (digital front end), phase compensation module, decimation block, filtering block and calibration module. The block diagram is shown as Fig 3.7.

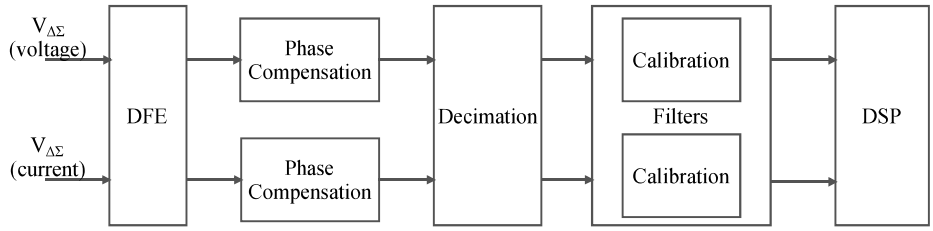

Figure 3.7: Block diagram of signal processing through digital front end

3.2.1 Digital front end

The converted sigma delta voltage and current signals feed digital front end (DFE). The DFE further synchronize and monitors the signals to be processed. The voltage and current signals are associated with status bit registers. If the DFE find that status bit registers are cleared, then instantaneous voltage and current values are set on negative or positive as per sigma-delta signals. Hence, the active power and energies are calculated using these values of voltage and current.

3.2.2 Decimation block

The decimation block reduces the sampling rate of the signals. It decimates three sigma delta signals obtained from voltage channels. The decimation ratio is set at 512 to provide parallel 24-bit data at frequency of 7.8125kHz.

3.2.3 Filters and calibration block

This block comprises of DC cancellation filter, rogowski coil integrater (ROC) and fundamental component filter and reactive filter. The use of DC cancellation filter is to remove DC components from voltage and current signals. ROC is selected as such to select the type of current sensing module. In the proposed work, the current sensing module is used is current transformer (CT). The fundamental component filter is actually low pass filter (LPF) which is used to calculate zero crossing, period, active and reactive energies. The output from reactive filter is used to calculate values of reactive power.

3.2.4 Digital Signal Processing

The output signal after being processed are fed into hardwired (digital signal processing) DSP for performing metering calculations. The DSP is used to perform metering operations such as signal measurement: RMS, period, zero- crossing, sag, swell and tamper. Each power signal corresponds to a energy register at every 7.8125kHz. These energy registers are up-down counters. The negative energy gets subtracted from positive energy when the accumulation is assigned to the energy registers.

3.3 Power Supply

The power supply module is used to provide power to the whole net metering circuit. In order to interface the 230V AC mains with the net energy meter, the AC supply is is stepped down and rectified using full wave bridge rectifier. Further, the output supply is smoothened using capacitors and ground potential is taken as a reference. The power supply meet the power demand of different units for example, the STPM34 controller circuit is operating at a voltage (V_{cc}) of 3.3V. Since the wired communication using UART is setup to transmit the data into the user interface, an isolated supply of 3.3V is also given to UART.

3.4 Microcontroller

The STPM34 microcontroller is used to metering operations in the net energy meter. The STPM34 is an ASSP (Application Specific Standard Product) which is purposefully designed for highly accurate metering. It is mixed signal integrated circuit consisting of an analog and digital module.The schematic diagram of STPM34 microcontroller is shown in Fig. 3.8. The analog module consists of 2^{nd} order 24-bit ADCs, two voltage references a

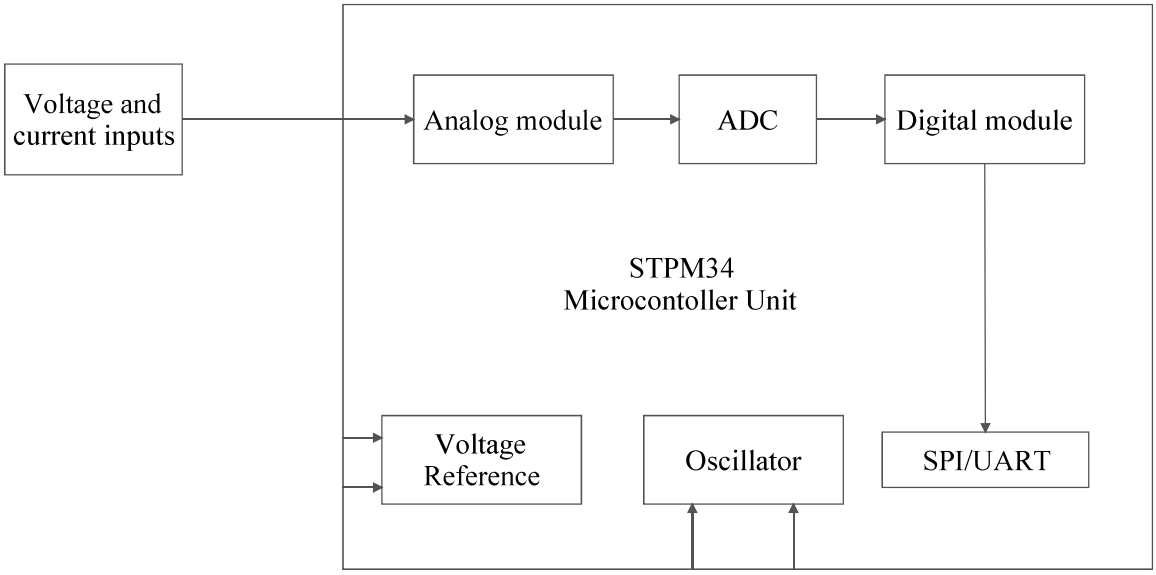

Figure 3.8: Microcontroller unit

voltage regulator and a buffer. The digital module consists of DFE(digital front end), hard-wired DSP and serial communication interface (SPI/UART). The utilization of all these features makes it ideal for single phase net metering.

3.4.1 Sigma delta ADC

STPM34 uses independent 2^{nd} order analog to digital converters to convert analog input voltage signals into a 24-bit corresponding digital signals. The performance of ADC is improved using dithering technique. This technique increases the effective range of signals for ADC conversion.

$$V_{\Delta\Sigma} = V_{line} * \frac{R_2}{R_1 + R_2} * \frac{A_V}{V_{ref}} \tag{3.10}$$

where, $V_{\Delta\Sigma}$ is the converted binary signal, A_V is the pre-amplification gain of value 2 and V_{ref} is the reference voltage set at 1.18V.

The sampling of signals is done by ADC and represented as output signals given as:

$$V_{RMS/phase} = \sqrt{\frac{1}{N}\int_{t_0}^{t_0+N} v(t)^2 dt} \tag{3.11}$$

$$I_{RMS/phase} = \sqrt{\frac{1}{N}\int_{t_0}^{t_0+N} i(t)^2 dt} \tag{3.12}$$

where, N = 200ms.

The converted signals are send to hardwired DSP which decimates and processes those signals in order to enhance the resolution and obtain all essential signal required for computation.

Chapter 4

Methodology Adopted

4.1 Software part of the net energy meter

This chapter includes the software design of net energy meter.The STPM34 is interfaced with 44 - pin STM8S207S6T6C microcontroller. It consists of two general purpose 16-bit timers TIM2 & TIM3 with 8-bit basic timer TIM4. The software module include the algorithms to fetch the data of various electrical parameters, like voltage, current, active, reactive and apparent power, active energy sent or received from the grid, from the STPM34 microcontroller.

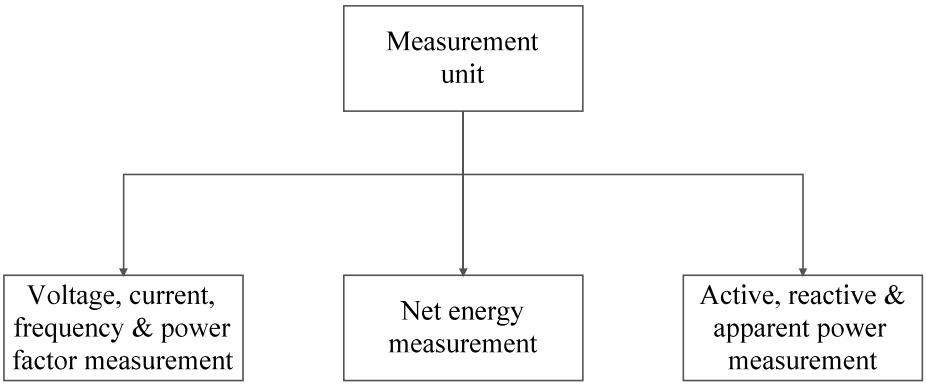

Figure 4.1: Software design for net energy meter

4.1.1 Configuring STPM34 energy metering IC

The algorithm 1. consists of the steps to configure the energy metering ic STPM34. With initialization of STPM34, communication peripherals are interfaced and data registers are read to calculate the desired parameters of net energy.

Algorithm 1 Configuring energy metering IC STPM34 to read data registers.

```
1. loop
2.     stpm_init(); // Initialization of STPM34 peripheral to select SPI communication.
3.     init_lcd(); // Initialization of LCD module to display parameters of net meter.
4.         CLK_SWCR = 0x02; // enable clock switch to HSE.
5.         CLK_SWR = 0xB4; //Switch to HSE Mod.
6.     Configure UART1 in Tx Mode for PC. //Baud rate = 9600 bps, 1 stop bit, no parity.
7.         UART1_BRR1 = 0x68;// UART_DIV for 9600@16MHz
8.     Configure SPI Module of micro-controller to communicate with STPM34 energy meter.
9.         SPI_CR1 = 0x27; //(0010 0111) //2-line unidir data mode, SSM enabled, SSI=1
10.        SPI_CR2 = 0x03; //(0000 0011) //SPE ENABLED
11.        SPI_CR1 = 0x40;
12.    Disable CRC.
13.    Enabling auto software latching.
14.    Set CT gain at 16.
15. end
```

When the STPM34 is initialized, SPI communication is set up with another micro-controller STM8S207S6T6C in order to read and receive the values of corresponding 32-bit data registers. In order to select SPI mode, SWC1 switches are put in off state and 10-pin FRC cable is connected to STM8S207S6T6C in order to enable transmission and receiving of data. Then, LCD module is initialized so as to display the instantaneous electrical parameters on LCD. The received values of data registers are used to calculate parameters of net meter. This data is further sent to PC via UART mode in order to store and analyze the data. In order to use UART port, SWC1 has to be on state. In addition to this, a separate 3.3V isolated supply has also been given to enable the UART port. To receive the values the UART is set at baud rate of 9600. The received data of the controller can be displayed on GUI/Hyperterminal/Evaluation software given by STmicroelectronics. The automatic software latching is enabled in STPM34 IC in order to extract transmission values at sampling rate.

4.1.2 Voltage, current, frequency and power factor measurement

The RMS voltage is sensed by voltage sensing circuit using voltage divider resisters where as RMS current is calculated by current sensing circuit using current transformer of ratio 1:2500. When the STPM34 is initialized and SPI communication is setup, the data registers are read. The values coming from the data registers are converted to decimal values and RMS values are calculated. After initialization of timer TIM2SR1, read and write requests are send to corresponding addresses to fetch the data from data registers. The register address 48 consists 32-bit data register containing Vrms data of 15-bit and Crms of 17-bit.

Algorithm 2 Measurement of voltage, current, frequency and power factor.

Input: Line voltage, current, phase delay.

Output: V_{RMS}, C_{RMS}, line frequency (f_{line}) and power factor

```
1. TIM2_SR1 = 0x00; // Initialize timer TIM2 for 1 second interrupt.
2. spi_transact_4bytesbuffer to read and write data from 32-bit data registers.
3.     SpiWriteBuffer[0] = 0x48; // Read register containing voltage and current data.
4.     SpiWriteBuffer[0] = 0x2E; // Read data register to get time period.
5. spi_transact_5bytesbuffer to read and write data for STPM34.
6. Initialize LCD and UART to display data. // Calculate values
7. loop
8.     Vrms = (test[2] & 0x00007FFF) * 0.0355; // Calculate RMS voltage.
9.     Crms = ((test[2] & 0xFFFF8000) >> 15) * 0.000268; // Calculate RMS current.
10.    frequency_raw = (test[1] & 0x00000FFF);
11.    frequency = 125000/frequency_raw; // Calculate line frequency.
12. end
```

The decimal values available from these registers is multiplied with LSB values to get measured values as given below:

$$V_{RMS} = [Dec_v] * LSB_{VRMS} \tag{4.1}$$

where LSB_{VRMS} = 0.0355 for voltage.

$$C_{RMS} = [Dec_i] * LSB_{CRMS} \tag{4.2}$$

where LSB_{CRMS} = 0.000268 for current. After reading RMS voltage and current, the frequency of the line is calculated. The time period of the voltage signal is calculated from zero crossing signal.

With the help of line period phase delay between voltage and current is calculated. This phase delay (ϕ) is stored in 12-bit data register and is used to find out the phase delay between voltage and current signals.

$$\phi = \frac{Phase\ delay * f_{line} * 360^{\circ}}{f_{clk}} \tag{4.3}$$

where, ϕ is the phase angle, f_{line} is line frequency and f_{clk} is the clock frequency. According to the definition of the power factor, it is defined as ratio of active power to apparent power and is given as:

$$p.f. = \frac{P_{calculated}}{S_{calculated}} \tag{4.4}$$

4.1.3 Measurement of active, reactive and apparent power

When the STPM34 is initialized and SPI communication is setup, the data registers are read. The values coming from the data registers are converted to decimal values and RMS values are calculated. After initialization of timer TIM2SR1, read and write requests are send to corresponding addresses to fetch the data from data registers. After calculating V_{RMS}, C_{RMS}, line frequency (f_{line}) and power factor(ϕ), these values are used to find the active power (P_{ACT}), reactive power (P_{REA}) and apparent power (P_{APP}). The values of active power, reactive power and apparent power is calculated as:

$$P_{act} = V_{\Sigma\Delta} * C_{\Sigma\Delta} * cos\phi * cali_v * cali_i \tag{4.5}$$

$$P_{rea} = V_{\Sigma\Delta} * C_{\Sigma\Delta} * cali_v * cali_i * sin\phi \tag{4.6}$$

$$P_{app} = V_{\Sigma\Delta} * C_{\Sigma\Delta} * cali_v * cali_i * \tag{4.7}$$

where,$V_{\Sigma\Delta}$ & $C_{\Sigma\Delta}$ is voltage and current after ADC conversion respectively, $cali_v$ & $cali_i$ are the calibration values set at 0.875.

The corresponding power registers store the measured values and calculated by multi-

Algorithm 3 Measurement of active power, reactive power and apparent power.

Input: V_{RMS}, C_{RMS}, line frequency (f_{line}) and power factor(ϕ).
Output: Active power (P_{act}), reactive power (P_{rea}) and apparent power (P_{app})

```
1. TIM2_SR1 = 0x00; // Initialize timer TIM2 for 1 second interrupt.
2. spi_transact_4bytesbuffer to read and write data from 32-bit data registers.
3.     SpiWriteBuffer[0] = 0x5C; // Read data register containing value of active power.
4.     SpiWriteBuffer[0] = 0x60; // Read data register to get the value of reactive power.
5.     SpiWriteBuffer[0] = 0x62; // Read data register to get the value of apparent power.
6. spi_transact_5bytesbuffer to read and write data for STPM34.
7. Initialize LCD and UART to display data. // Calculate values
8. loop
9.     power_sign = (char)(test[0] & 0x0000000F); // To check the sign of active power.
10.    active_power = (active_power * 1.52)/(10000); // Calculate P_act.
11.    reactive_power = (reactive_power * 1.52)/(10000); // Calculate P_rea.
12.    apparent_power = (apparent_power * 1.52)/(10000);// Calculate P_app.
13. end
```

plying decimal values with LSB values.

$$P_{act} = [Dec_{act}] * LSB_{act} \tag{4.8}$$

where, LSB_{act} = 1.52 * 10^{-4}

$$P_{rea} = [Dec_{rea}] * LSB_{rea} \tag{4.9}$$

where, LSB_{rea} = 1.52 * 10^{-4}

$$P_{app} = [Dec_{app}] * LSB_{app} \tag{4.10}$$

where, LSB_{app} = 1.52 * 10^{-4}

4.1.4 Measurement of net energy, import energy and export energy

Once the voltage, current, frequency and power factor is calculated, those values are used to find out the energy parameters. The energy metering IC STPM34 is used to find the

net energy, import energy and export energy. The power sign indicates the sign of energy whether it is positive or negative which determines the flow of power on the line. Then net energy is calculated by multiplying the decimal value obtained from energy register with LSB value given as:

$$E_{net} = [Decimalvalue] * LSB_{net} \tag{4.11}$$

where, LSB_{net} = 111 *10^{-13}

$$E_{in} = [Decimalvalue] * LSB_{in} \tag{4.12}$$

where, LSB_{in} = 111 *10^{-13}

$$E_{out} = [Decimalvalue] * LSB_{out} \tag{4.13}$$

where, LSB_{out} = 111 *10^{-13}

Algorithm 4 Measurement of net energy, import energy and export energy.

Input: Active power (P_{ACT}), reactive power (P_{REA}) and apparent power (P_{APP})
Output: net energy (E_{net}) , import energy (E_{in}) and export energy (E_{out})

```
1.  TIM2_SR1 = 0x00; // Initialize timer TIM2 for 1 second interrupt.
2.  spi_transact_4bytesbuffer to read and write data from 32-bit data registers.
3.      SpiWriteBuffer[0] = 0x2A; // Read data register containing sign of net active energy.
4.      SpiWriteBuffer[0] = 0x54; // Read data register to get the value of net active energy. .
5.  spi_transact_5bytesbuffer to read and write data for STPM34.
6.  Initialize LCD and UART to display data. // Calculate values
7.  loop
8.      power_sign = (char)(test[0] & 0x0000000F); // To check the sign of active energy.
9.      Net energy = ((Dec value * 111.0) /1000000)/10000000 // Calculate net energy.
10.       if (Last measured energy < Net energy) then
11.       Energy import = net_energy − last measured energy;
12.       else if (Last measured energy > net_energy) then
13.       Energy export = last measured energy − net_energy;
14.      else last measured energy = net_energy;
15.       Total net energy = Energy import - Energy export;
16. end
```

Chapter 5

Results and Discussions

In context of achieving the objective of validating accurate measurements of proposed net meter, an experimental setup was conducted in renewable energy lab at Thapar University, Patiala. The main aim of the experiment was to demonstrate the working of proposed net energy meter and calculate the net energy units. In order to determine accuracy, percentage error has been calculated by comparing actual values and measured values. An algorithm is developed in embedded C to find the net exchange of units using IAR embedded work-bench. Furthermore, the net meter gives negative sign if energy is being injected into the grid.

5.1 Accuracy of voltage measurement

The input voltage while measuring, is varied between 224V - 230V by changing the load and net energy meter measured the output values. The measured voltage from the net energy meter is compared with voltage displayed by multimeter. The error percentage was

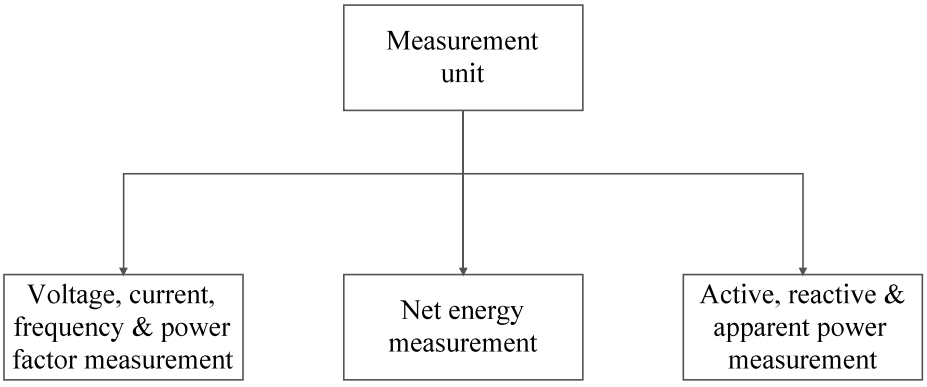

Figure 5.1: Software design for net energy meter

calculated and is found to be not more than 0.4%. Hence, it meets the IS standards set for single phase AC energy meter.

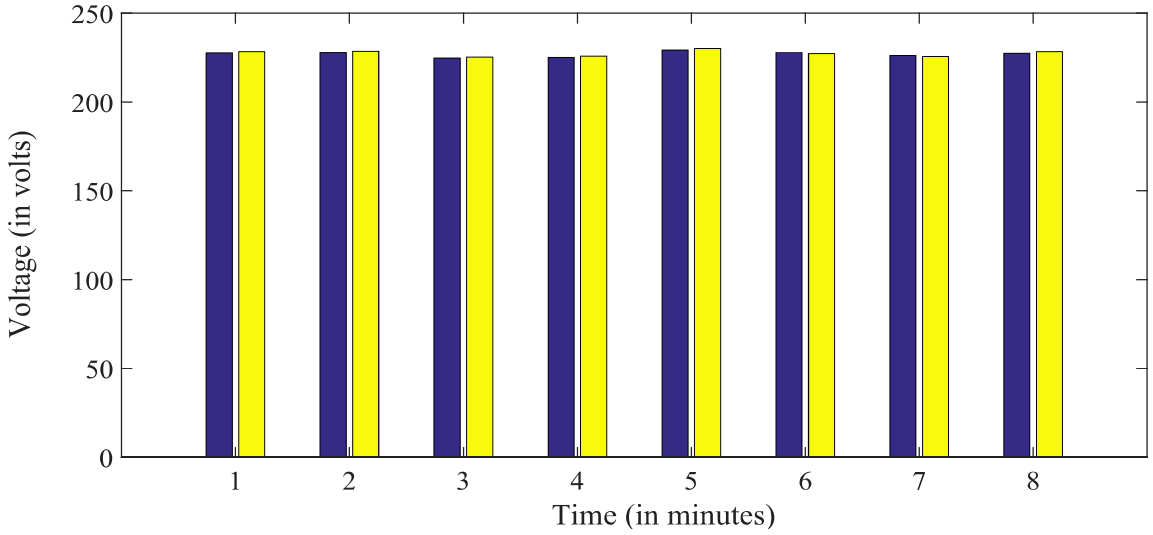

Figure 5.2: Accuracy of voltage measurement by net meter

Table 5.1: Accuracy of voltage measured on resistive load

S. No.	Actual voltage (RMS)	Measured voltage (RMS)	Maximum error (in %)
1.	227.6 V	228.4 V	0.3515
2.	227.8 V	228.5 V	0.3073
3.	224.7 V	225.3 V	0.2670
4.	225.1 V	225.9 V	0.3554
5.	229.3 V	230.2 V	0.3925
6.	227.9 V	227.2 V	0.3072
7.	226.2 V	225.7 V	0.2215
8.	227.5 V	228.3 V	0.3516

5.2 Accuracy of frequency measurement

Once the accuracy of voltage measurement is tested, the test for accurate measurement for frequency variations is conducted by varying frequency between 48 Hz - 51 Hz. The change in frequency was produced by causing variations in the resistive load and effect on frequency was observed. The error percentage was calculated and is found to be not more that 0.4%. Thus, a very good accuracy in results is achieved.

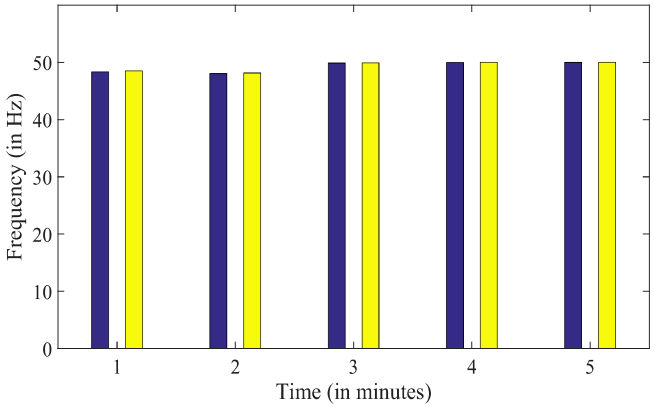

Figure 5.3: Accuracy of frequency measurement

Table 5.2: Accuracy of frequency measurement on resistive load

S. No.	Actual frequency	Measured frequency	Maximum error (in %)
1.	48.34 Hz	48.53 Hz	0.3931
2.	48.04 Hz	48.15 Hz	0.2283
3.	49.88 Hz	49.92 Hz	0.07998
4.	49.98 Hz	50.02 Hz	0.08
5.	50.00 Hz	50.04 Hz	0.08

5.3 Tests for bidirectional metering of net energy meter.

The proposed hardware design of net meter is tested to measure the net units and send the metering data to the PC for monitoring of energy. In net energy metering, when the power is offset to the utility from the consumer side, it is used to meet the load requirement of local area. At this point of time, the utility acts a load where as consumer act as a producer of electricity. A similar type of environment for net metering was tried to be constructed in renewable energy lab. The sole objective of setting up such an environment was to test the proposed net energy meter for the bi-directional energy metering.

A 24-hour (12:30 am - 11:30 pm) analysis of day was taken under consideration and net energy was calculated after every hour. The net energy was found to be capable of measuring active, reactive and apparent power accurately. Moreover, the values were recorded for imported and exported energy and net units were calculated simultaneously. The whole set of values are monitored on PC using UART communication.

5.3.1 Measurement of different parameters of energy metering

A time duration of 24 hours of the day has been considered and various parameters are measured during this time. The load variation almost resembles the real time load pattern of residential consumers and based on which results has been procured. To monitor the impact of net metering in results, two scenarios were taken into consideration as given:

- **Scenario - 1** When the energy is imported from the grid. In this scenario, a resistive load was used and varied at different time intervals. The time duration for the observation of results was fixed from 12:30 am - 09:30 am and 6:30 pm to 11:30 pm. The imported energy is represented as E_{in} and is measured in Kwh as shown on net meter and PC.

- **Scenario - 2** When the energy is exported to the grid. In this scenario, load side acts as producers of energy and utility would act as a consumer of energy. Hence, the direction of energy flowing through the line would in reverse direction i.e. from load to utility. The time duration of the observation of the results was fixed from 10:30 am to 5:30 pm. The exported energy is represented as E_{out} and is measured in Kwh as shown on net meter and PC.

In the end, net energy represented as E_{net} is calculated as:

$$E_{net} = E_{in} - E_{out} \tag{5.1}$$

5.3.2 Measurement of Voltage and current vs time

The test of voltage vs time was conducted in the laboratory where the change in voltage was observed by causing variation in the load. A resistive load of 1 kW approx was used which was varied during each hour of the day. The Table no. 5.3 shows variations in voltage w.r.t time were recorded and observed as shown in Fig 5.4. The voltage remained almost constant with the change in load.

The test of current vs time was conducted in the laboratory where the change in current was observed by causing variation in the load. A resistive load of 1 kW approx was used which was varied during each hour of the day. The Table no. 5.4 shows variations in voltage w.r.t time were recorded and observed as shown in Fig 5.5. The negative sign of the current represents that the energy is being injected into the grid. While measuring power, voltage signal is taken as reference to find the direction of current through the line.

Table 5.3: Measurement of RMS voltage w.r.t time

Time	RMS voltage
12:30 AM	229.3 V
01:30 AM	229.4 V
02:30 AM	229.9 V
03:30 AM	229.7 V
04:30 AM	229.8 V
05:30 AM	229.7 V
06:30 AM	228.7 V
07:30 AM	228.2 V
08:30 AM	229.9 V
09:30 AM	229.7 V
10:30 AM	229.6 V
11:30 AM	228.9 V
12:30 PM	228.4 V
01:30 PM	227.9 V
02:30 PM	228.1 V
03:30 PM	227.8 V
04:30 PM	229.3 V
05:30 PM	229.4 V
06:30 PM	229.9 V
07:30 PM	229.7 V
08:30 PM	229.6 V
09:30 PM	228.9 V
10:30 PM	228.4 V
11:30 PM	227.9 V

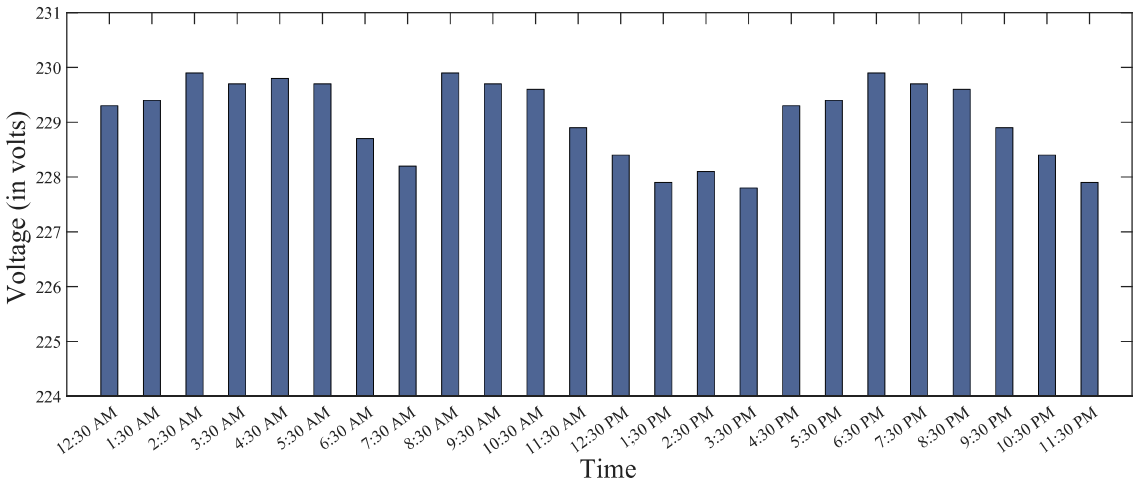

Figure 5.4: Variation of voltage w.r.t time due to change in load

Table 5.4: Measurement of RMS current w.r.t time

Time	RMS current
12:30 AM	1.5 A
01:30 AM	1.6 A
02:30 AM	0.8 A
03:30 AM	0.8 A
04:30 AM	0.8 A
05:30 AM	0.8 A
06:30 AM	2.3 A
07:30 AM	3.1 A
08:30 AM	3.8 A
09:30 AM	3.8 A
10:30 AM	-1.6 A
11:30 AM	-1.6 A
12:30 PM	-1.6 A
01:30 PM	-3.1 A
02:30 PM	-3.8 A
03:30 PM	-3.8 A
04:30 PM	-3.1 A
05:30 PM	-1.5 A
06:30 PM	1.5 A
07:30 PM	2.3 A
08:30 PM	3.1 A
09:30 PM	3.8 A
10:30 PM	3.8 A
11:30 PM	3.8 A

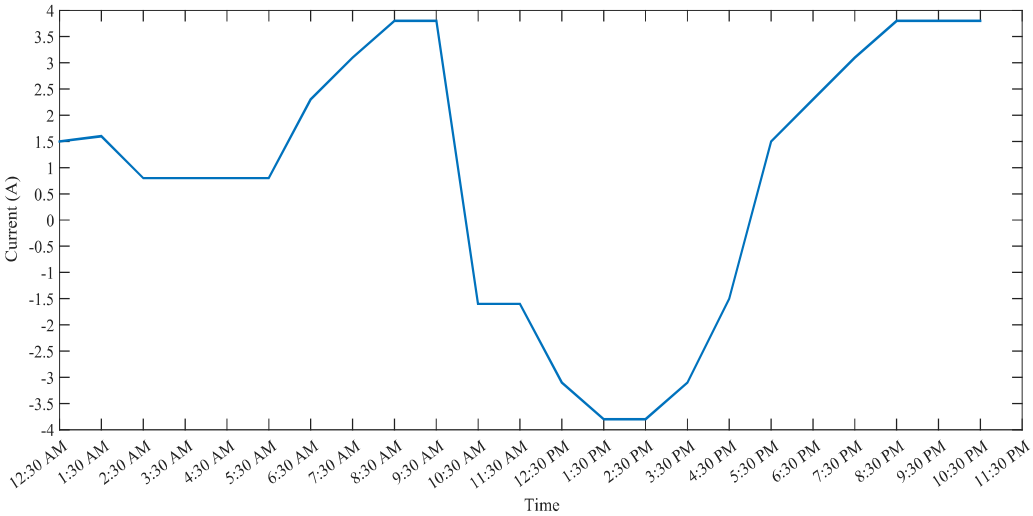

Figure 5.5: Measurement of current w.r.t time

5.3.3 Measurement of frequency and power factor w.r.t change in load

The change in frequency was tested for change in load and it was found that it remain practically almost constant for variations in the load. The load was varied from 175 W to 870 W and change in frequency was recorded. The table no. 5.5 shows variations in voltage w.r.t time were recorded and observed as shown in Fig 5.6. Since, the load is resistive in nature, the value of power factor ranges between 0.991- 0.999.

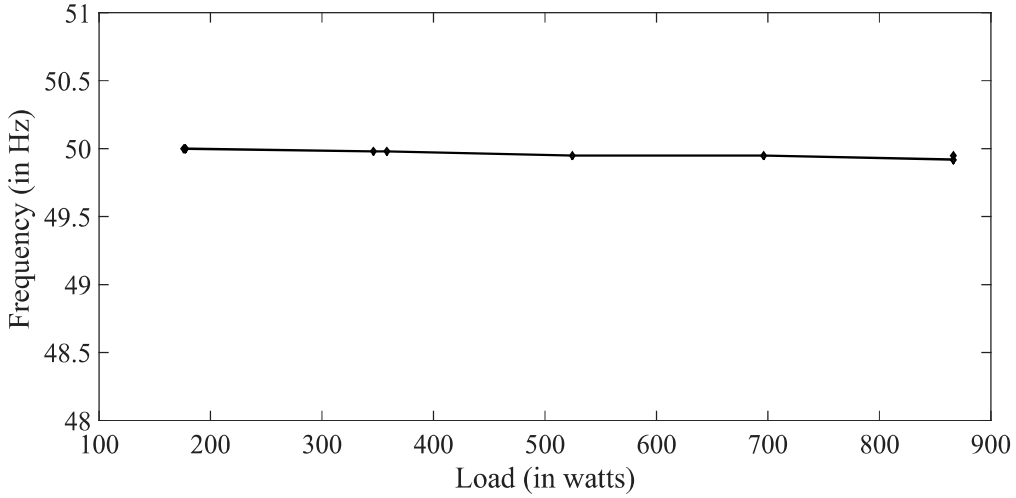

Figure 5.6: Measurement of frequency w.r.t change in load

Table 5.5: Measurement of frequency w.r.t change in load

Load (watts)	Frequency
177.41 W	50 Hz
175.75 W	50 Hz
177.80 W	50 Hz
176.52 W	50 Hz
346.32 W	49.98 Hz
357.99 W	49.98 Hz
524.94 W	49.95 Hz
696.29 W	49.95 Hz
866.19 W	49.92 Hz
866.59 W	49.95 Hz

5.3.4 Measurement of reactive power, active power and apparent power

The net energy meter measures reactive power, active power and apparent power for both scenarios as described in section 5.3.1. Based on calculated voltage, current and power factor, powers were calculated for time period of 24 hours and change in power was observed

with the change in load as well as when energy is exported to grid. The negative sign of power signifies the energy being transmitted to the utility. Based on the calculations of reactive power (P_{rea}), active power (P_{act}) and apparent power (P_{app}), results are observed and plotted. In Fig 5.7, reactive power (P_{rea}) values are plotted as shown in table 5.6. However, active power (P_{act}) measured for an interval of 24 hours in shown in Fig 5.8 and values are retrieved as shown in Table 5.7.

Table 5.6: Measurement of reactive power w.r.t time

Time	Reactive power
12:30 AM	3.11 VAR
01:30 AM	8.21 VAR
02:30 AM	1.98 VAR
03:30 AM	1.94 VAR
04:30 AM	2.16 VAR
05:30 AM	3.17 VAR
06:30 AM	6.68 VAR
07:30 AM	9.38 VAR
08:30 AM	8.79 VAR
09:30 AM	6.79 VAR
10:30 AM	-8.87 VAR
11:30 AM	-7.02 VAR
12:30 PM	-8.02 VAR
01:30 PM	-16.13 VAR
02:30 PM	-14.47 VAR
03:30 PM	-11.18 VAR
04:30 PM	-7.16 VAR
05:30 PM	-4.56 VAR
06:30 PM	3.43 VAR
07:30 PM	7.55 VAR
08:30 PM	7.78 VAR
09:30 PM	6.56 VAR
10:30 PM	8.80 VAR
11:30 PM	9.68 VAR

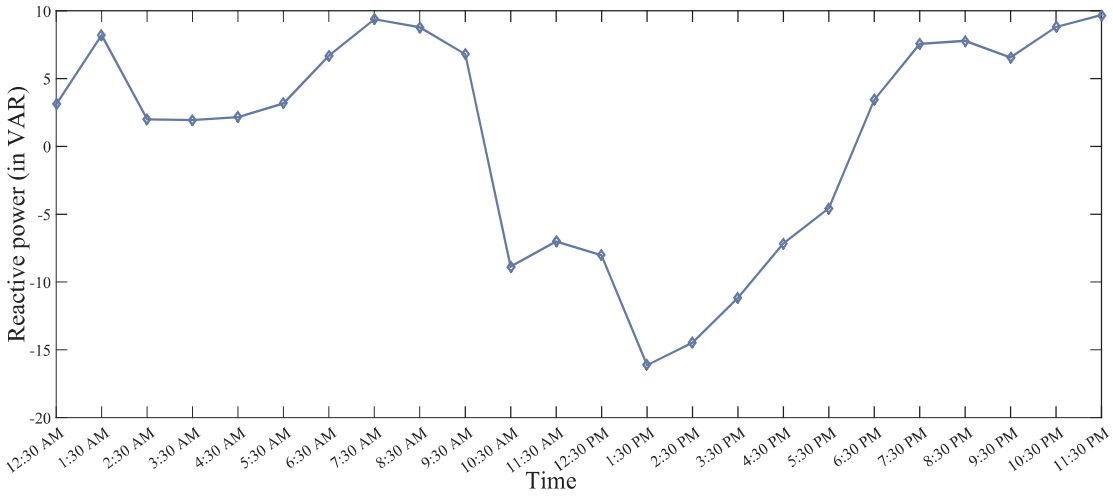

Figure 5.7: Measurement of reactive power w.r.t change in load

Table 5.7: Measurement of active power w.r.t time

Time	Active power
12:30 AM	346.32 W
01:30 AM	357.99 W
02:30 AM	177.41 W
03:30 AM	177.51 W
04:30 AM	177.80 W
05:30 AM	176.52 W
06:30 AM	524.94 W
07:30 AM	696.29 W
08:30 AM	866.19 W
09:30 AM	866.59 W
10:30 AM	-358.91 W
11:30 AM	-358.18 W
12:30 PM	-359.40 W
01:30 PM	-708.18 W
02:30 PM	-872.24 W
03:30 PM	-867.06 W
04:30 PM	-694.28 W
05:30 PM	-361.68 W
06:30 PM	350.11 W
07:30 PM	527.47 W
08:30 PM	694.35 W
09:30 PM	864.04 W
10:30 PM	866.11 W
11:30 PM	869.61 W

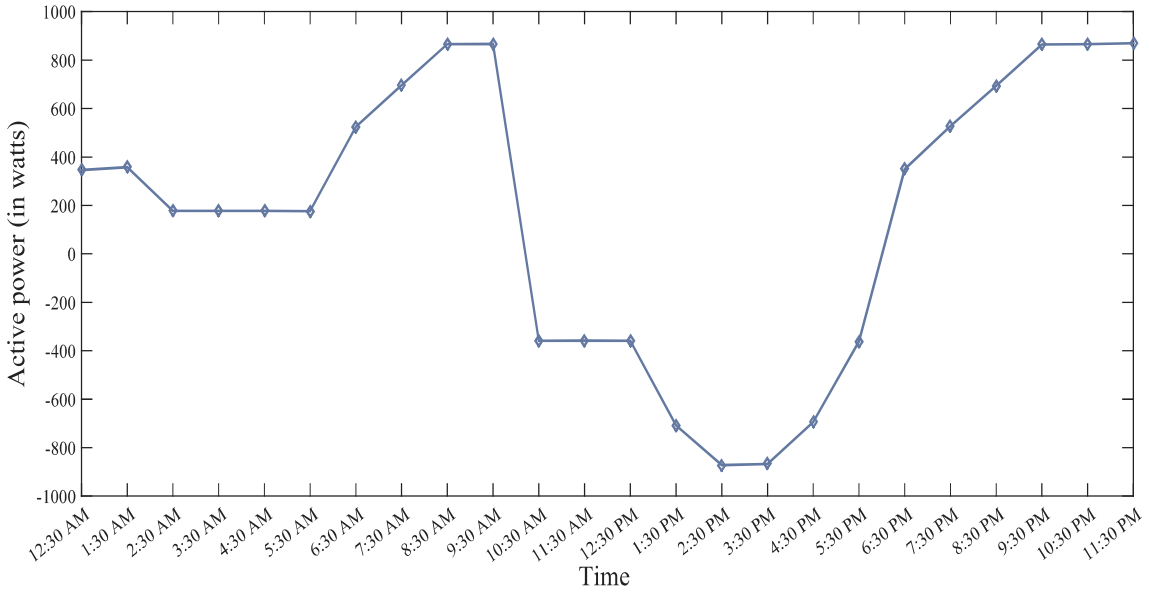

Figure 5.8: Measurement of active power w.r.t change in load

Table 5.8: Measurement of apparent power w.r.t time

Time	Apparent power
12:30 AM	349.30 VA
01:30 AM	356.22 VA
02:30 AM	178.51 VA
03:30 AM	178.63 VA
04:30 AM	178.81 VA
05:30 AM	176.71 VA
06:30 AM	527.27 VA
07:30 AM	699.46 VA
08:30 AM	874.92 VA
09:30 AM	874.42 VA
10:30 AM	356.50 VA
11:30 AM	356.68 VA
12:30 PM	357.04 VA
01:30 PM	703.21 VA
02:30 PM	874.06 VA
03:30 PM	871.96 VA
04:30 PM	699.69 VA
05:30 PM	353.53 VA
06:30 PM	352.52 VA
07:30 PM	528.48 VA
08:30 PM	699.09 VA
09:30 PM	873.06 VA
10:30 PM	873.47 VA
11:30 PM	873.85 VA

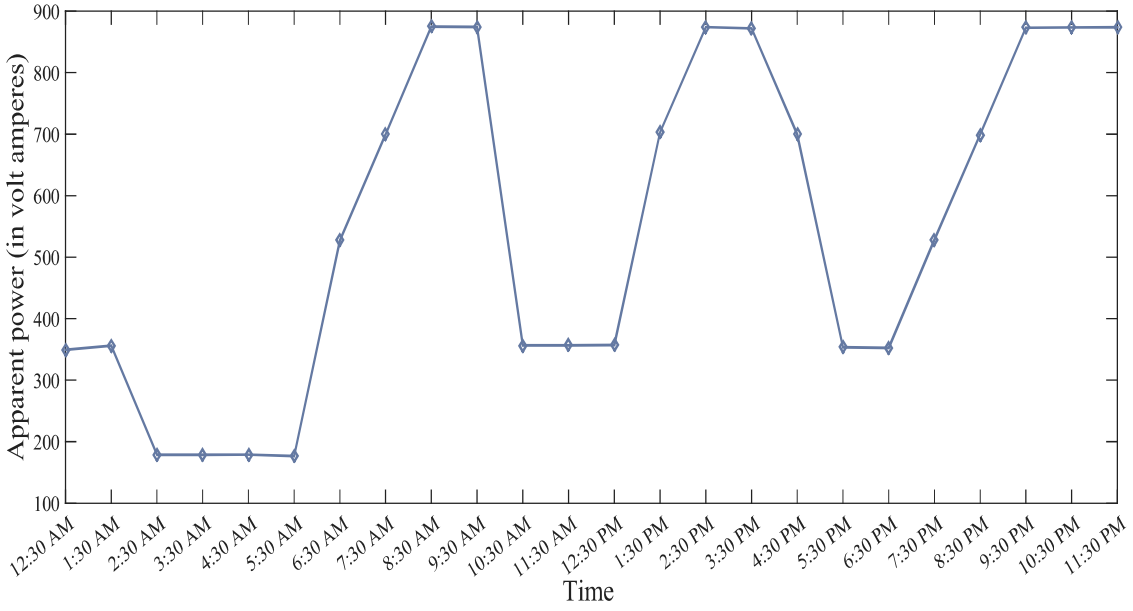

Figure 5.9: Measurement of apparent power w.r.t change in load

The apparent power (P_{app}) is defined as combination of active power (P_{act}) and reactive power (P_{rea}) and is calculated as volt-amperes by net energy meter. Table 5.8 depicts the variation in apparent power w.r.t time due to change in load and values are plotted in Fig 5.9.

5.3.5 Measurement of imported energy, exported energy and net energy

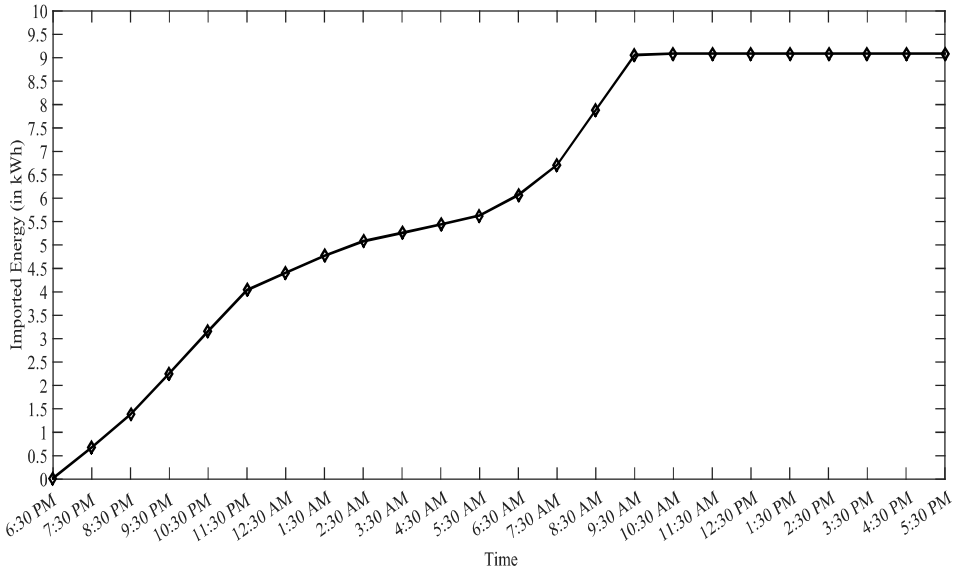

Figure 5.10: Measurement of imported energy

The proposed net meter continuously measures the power flowing through the line in both directions. Based on the two scenarios as described in section 5.3.1, the results are calculated. The import of energy is represented as E_{in} where as export of energy is defined as E_{out} with unit in kWh. During 12:30 am to 9:30 am and 06:30 pm to 11:30 pm, the load demand is met through energy imported from the grid. The net meter measures the imported energy and values are displayed on the LCD.

Table 5.9: Measurement of imported energy

Time	Imported energy
06:30 PM	0.02 KWh
07:30 PM	0.68 KWh
08:30 PM	1.38 KWh
09:30 PM	2.26 KWh
10:30 PM	3.16 KWh
11:30 PM	4.04 KWh
12:30 AM	4.41 KWh
01:30 AM	4.77 KWh
02:30 AM	5.08 KWh
03:30 AM	5.26 KWh
04:30 AM	5.44 KWh
05:30 AM	5.63 KWh
06:30 AM	6.07 KWh
07:30 AM	6.71 KWh
08:30 AM	7.89 KWh
09:30 AM	9.06 KWh
10:30 AM	9.09 KWh
11:30 AM	9.09 KWh
12:30 PM	9.09 KWh
01:30 PM	9.09 KWh
02:30 PM	9.09 KWh
03:30 PM	9.09 KWh
04:30 PM	9.09 KWh
05:30 PM	9.09 KWh

The energy imported per hour could be calculated by subtracting imported energy at T_1 time interval from imported energy at T_2 time interval. Table 5.19 shows the energy exported to grid at different time intervals. During the time duration 10:30 am to 05:30 pm, when the excess energy is available, the utility acts as consumer for electric energy whereas load side acts producer of electricity. Thus, a consumer acts a producer of electricity on one side and producer acts as consumer of electricity on the other side. To measure the bi-directional flow of energy, the load was connected on supply side and load side was given

the supply.

Table 5.10: Measurement of energy exported to utility.

Time	Exported energy
06:30 PM	0.00 KWh
07:30 PM	0.00 KWh
08:30 PM	0.00 KWh
09:30 PM	0.00 KWh
10:30 PM	0.00 KWh
11:30 PM	0.00 KWh
12:30 AM	0.00 KWh
01:30 AM	0.00 KWh
02:30 AM	0.00 KWh
03:30 AM	0.00 KWh
04:30 AM	0.00 KWh
05:30 AM	0.00 KWh
06:30 AM	0.00 KWh
07:30 AM	0.00 KWh
08:30 AM	0.00 KWh
09:30 AM	0.00 KWh
10:30 AM	0.34 KWh
11:30 AM	0.62 KWh
12:30 PM	1.12 KWh
01:30 PM	1.76 KWh
02:30 PM	2.56 KWh
03:30 PM	3.44 KWh
04:30 PM	3.99 KWh
05:30 PM	4.43 KWh

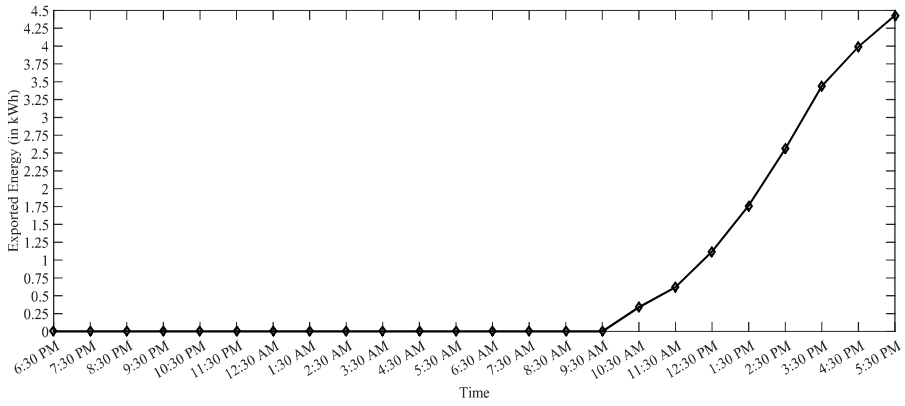

Figure 5.11: Measurement of exported energy

Thus, the net meter starts decrementing the energy units when there is export of energy from load side to utility. The energy exported per hour could be calculated by subtracting exported energy at T_1 time interval from exported energy at T_2 time interval. Table 5.10 shows the energy exported to grid at different time intervals. To enhance the accuracy while plotting the graph, the units of energy are taken as watt-hour instead of kilowatt-hour.

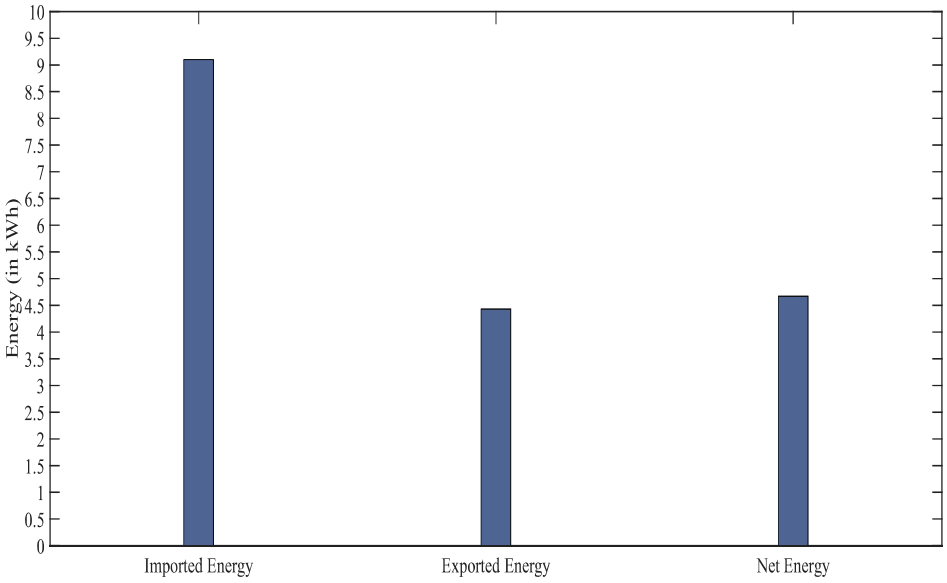

Figure 5.12: Analysis of energy savings

The net meter records the both imported and exported energy and calculates the net energy based on them. At any interval of the day, the readings are available for imported energy, exported energy as well as net energy. As significant from the results, the net energy metering contribute to greater energy savings and thus reduced costs of the electricity bills. In addition to it, integration of renewable resources on the consumer side reduces the burden on the electrical infrastructure and encourages the use of green energy.

5.4 Hardware implementation

The hardware implementation is done at Renewable lab, Thapar University, Patiala. STM8S acts master controller and fetch data from the STPM34 controller and displays data on LCD. Ardunio is used to act as UART to PC communication mode.

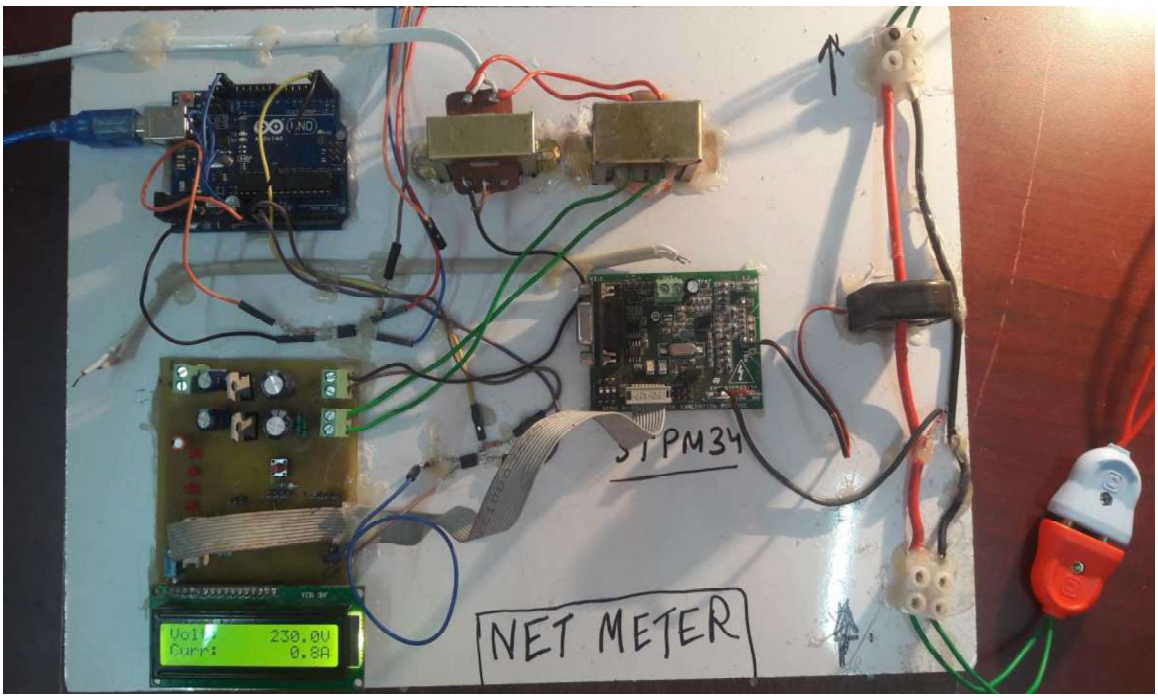

Figure 5.13: Hardware setup for net energy meter

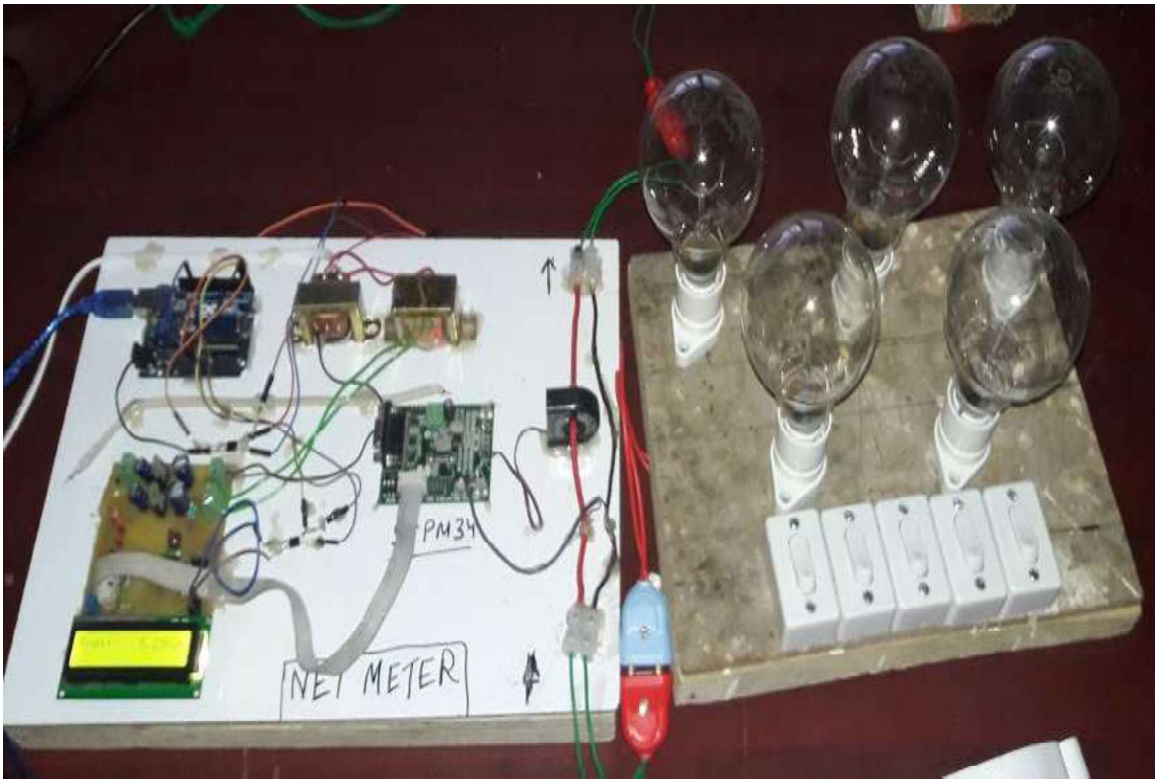

Figure 5.14: Experimental setup for net energy meter demonstration

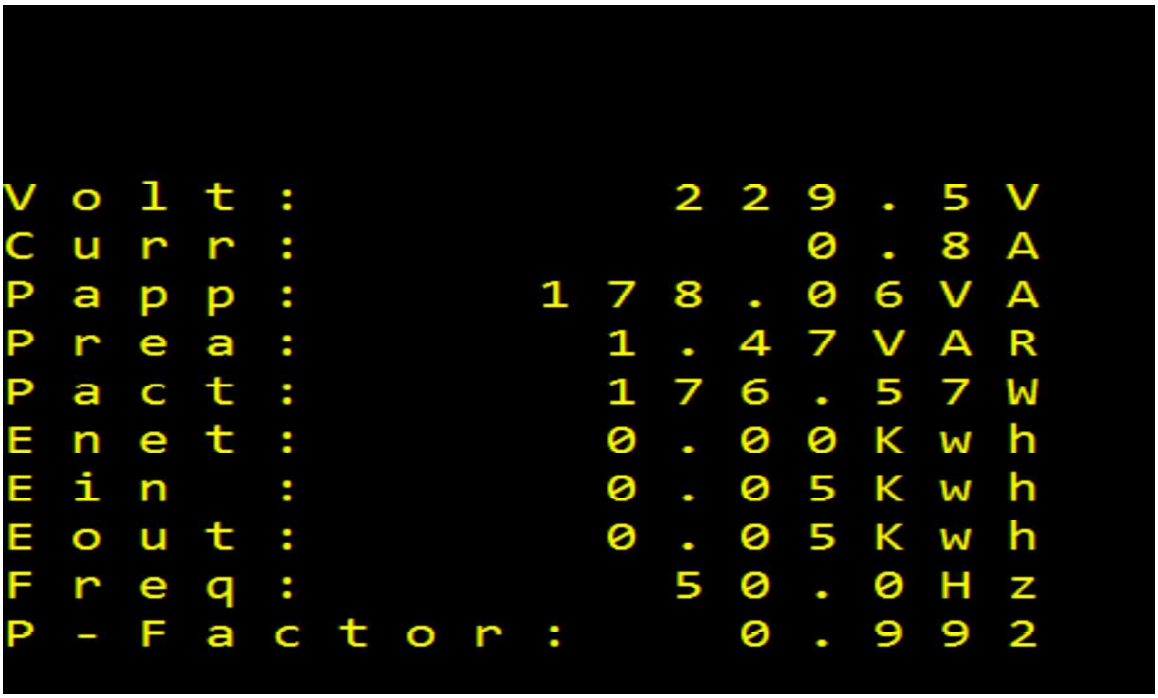

Figure 5.15: Data displayed on GUI via UART transmission

5.5 Discussion

- The results for bi-directional flow of energy were obtained over a wide variation in the load.
- The results clearly depicted the energy savings for the case of net metering. Thus, it encourages the consumers towards the green energy and significantly reducing burden on the utility.
- In addition to savings in energy units, the billing costs are significantly reduced as per billing system at different places.
- The use of bi-directional meter eliminates the use of two uni-directional meters used for measuring imported and exported energy.
- The energy metering IC STPM34 brings out the novelty, to enrich it more features keeping this dissertation as the reference.
- The net energy meter meets the IEC 62053, ANSI 12.2 standards for AC watt meters.

Chapter 6

Conclusions & Future Scope

6.1 Conclusion

The electrical network is bound to disturbances such as frequency variations, overloading of the grid and cascading blackouts. The main reason of all these disturbances is the mismatch between generation and load demand. Net energy metering offers consumer friendly solution by urging them to fulfill their peak load through installed solar generation rather than using utility supply. Thus, the dissertation is summarized as following:

- In this dissertation concept of net metering using rooftop SPV system has been analyzed.
- In addition to this, a novel hardware design of net energy meter based on STPM34 metering IC has also been proposed.
- The working of net meter was tested using a resistive load of 1 kW and readings were noted.
- The data from STPM34 was imported to PC by using UART interface and all the values were monitored.
- This data can be stored in the form of excel sheet using the evaluation software and can used by utility for different purposes such as load forecasting, load monitoring and remote connection/disconnection.

6.2 Future Scope

Further, the work could be extended for enabling the net energy meter with features of IoT due to its adaptive nature in any type of environment. The data transmission in this energy meter is based on wired connection with UART interface. In future, the net meter could be interfaced with wifi/RF module. The STPM34 could be further explored and put to use to find out the power quality parameters such voltage sag, swell and overcurrent. The future scope of the net energy meter includes its integration with the smart home energy management systems. It can be used to control smart appliances of the smart buildings by the consumer as well as utility for implementation of load optimization techniques. In addition, this dissertation has tried to create a corridor for the extensive use of renewable energy sources at consumer side and conserving the nature and energy sources.

BIBLIOGRAPHY

[1] L. Jia and L. Tong, "Renewables and storage in distribution systems: Centralized vs. decentralized integration," *IEEE Journal on Selected Areas in Communications*, vol. 34, no. 3, pp. 665–674, March 2016.

[2] G. Xu, W. Yu, D. Griffith, N. Golmie, and P. Moulema, "Toward integrating distributed energy resources and storage devices in smart grid," *IEEE Internet of Things Journal*, vol. 4, no. 1, pp. 192–204, Feb 2017.

[3] B. A. Carreras, D. E. Newman, I. Dobson, and A. B. Poole, "Evidence for self-organized criticality in a time series of electric power system blackouts," *IEEE Transactions on Circuits and Systems I: Regular Papers*, vol. 51, no. 9, pp. 1733–1740, Sept 2004.

[4] J. S. John. India's massive blackout calls for smarter grid. [Online]. Available: https://www.greentechmedia.com/articles/read/indias-massive-blackout-calls-for-smarter-grid-from-the-bottom-up

[5] J. Reilly. Blackout in india. [Online]. Available: http://www.dailymail.co.uk/news/article-2181517/Indias-power-grid-fails-second-day-running-600-million-people-endure-blackout.html

[6] Y. Yan, Y. Qian, H. Sharif, and D. Tipper, "A survey on smart grid communication infrastructures: Motivations, requirements and challenges," *IEEE Communications Surveys Tutorials*, vol. 15, no. 1, pp. 5–20, First 2013.

[7] X. Fang, S. Misra, G. Xue, and D. Yang, "Smart grid x2014; the new and improved power grid: A survey," *IEEE Communications Surveys Tutorials*, vol. 14, no. 4, pp. 944–980, Fourth 2012.

[8] D. G. Hart, "Using ami to realize the smart grid," in *2008 IEEE Power and Energy Society General Meeting - Conversion and Delivery of Electrical Energy in the 21st Century*, July 2008, pp. 1–2.

[9] R. R. Mohassel, A. Fung, F. Mohammadi, and K. Raahemifar, "A survey on advanced metering infrastructure," *International Journal of Electrical Power & Energy Systems*, vol. 63, pp. 473–484, 2014.

[10] C. W. Potter, A. Archambault, and K. Westrick, "Building a smarter smart grid through better renewable energy information," in *2009 IEEE/PES Power Systems Conference and Exposition*, March 2009, pp. 1–5.

[11] A. J. D. Rathnayaka, V. M. Potdar, T. S. Dillon, O. K. Hussain, and E. Chang, "A methodology to find influential prosumers in prosumer community groups," *IEEE Transactions on Industrial Informatics*, vol. 10, no. 1, pp. 706–713, Feb 2014.

[12] A. C. Luna, N. L. Diaz, M. Graells, J. C. Vasquez, and J. M. Guerrero, "Cooperative energy management for a cluster of households prosumers," *IEEE Transactions on Consumer Electronics*, vol. 62, no. 3, pp. 235–242, August 2016.

[13] A. Poullikkas, "A comparative assessment of net metering and feed in tariff schemes for residential pv systems," *Sustainable Energy Technologies and Assessments*, vol. 3, pp. 1–8, 2013.

[14] A. Campoccia, L. Dusonchet, E. Telaretti, and G. Zizzo, "Comparative analysis of different supporting measures for the production of electrical energy by solar pv and wind systems: Four representative european cases," *Solar Energy*, vol. 83, no. 3, pp. 287–297, 2009.

[15] K. Sedghisigarchi, "Residential solar systems: Technology, net-metering, and financial payback," in *2009 IEEE Electrical Power Energy Conference (EPEC)*, Oct 2009, pp. 1–6.

[16] S. D. Dunlap, W. B. Morrow, and J. F. Timte, "Bidirectional metering and control of electric energy between the power grid and vehicle power systems," Oct. 6 2008, uS Patent App. 12/287,105.

[17] J. A. Momoh, "Smart grid design for efficient and flexible power networks operation and control," in *2009 IEEE/PES Power Systems Conference and Exposition*, March 2009, pp. 1–8.

[18] A. Mishra, D. Irwin, P. Shenoy, J. Kurose, and T. Zhu, "Greencharge: Managing renewableenergy in smart buildings," *IEEE Journal on Selected Areas in Communications*, vol. 31, no. 7, pp. 1281–1293, July 2013.

[19] H. Kanchev, D. Lu, F. Colas, V. Lazarov, and B. Francois, "Energy management and operational planning of a microgrid with a pv-based active generator for smart grid applications," *IEEE Transactions on Industrial Electronics*, vol. 58, no. 10, pp. 4583–4592, Oct 2011.

[20] A. Poullikkas, G. Kourtis, and I. Hadjipaschalis, "A review of net metering mechanism for electricity renewable energy sources," *Int. J. Energy Environ*, vol. 4, no. 6, pp. 975–1002, 2013.

[21] T. E. D. Carpio-Huayllas, D. S. Ramos, and R. L. Vasquez-Arnez, "Feed-in and net metering tariffs: An assessment for their application on microgrid systems," in *2012 Sixth IEEE/PES Transmission and Distribution: Latin America Conference and Exposition (T D-LA)*, Sept 2012, pp. 1–6.

[22] N. R. Darghouth, G. Barbose, and R. Wiser, "The impact of rate design and net metering on the bill savings from distributed pv for residential customers in california," *Energy Policy*, vol. 39, no. 9, pp. 5243–5253, 2011.

[23] Y. Ru, J. Kleissl, and S. Martinez, "Storage size determination for grid-connected photovoltaic systems," *IEEE Transactions on Sustainable Energy*, vol. 4, no. 1, pp. 68–81, Jan 2013.

[24] T. Tony, P. Sivraj, and K. K. Sasi, "Net energy meter with appliance control and bi-directional communication capability," in *2016 International Conference on Advances in Computing, Communications and Informatics (ICACCI)*, Sept 2016, pp. 2650–2653.

[25] V. Snram, S. A. Nivass, and C. Selvam, "Bi-directional energy meters and remote monitoring of energy nodes using lonworks technology," in *2012 4th International Conference on Intelligent and Advanced Systems (ICIAS2012)*, vol. 2, June 2012, pp. 536–539.

[26] K. Maharaja, P. P. Balaji, S. Sangeetha, and M. Elakkiya, "Development of bidirectional net meter in grid connected solar pv system for domestic consumers," in *2016 International Conference on Energy Efficient Technologies for Sustainability (ICEETS)*, April 2016, pp. 46–49.

[27] Z. Li and B. Lianping, "Research about bi-directional electronic energy meter and power quality analyzers," in *2013 Third International Conference on Instrumentation, Measurement, Computer, Communication and Control*, Sept 2013, pp. 1323–1327.

[28] T. K. Kwang and S. Masri, "Single phase grid tie inverter for photovoltaic application," in *2010 IEEE Conference on Sustainable Utilization and Development in Engineering and Technology*, Nov 2010, pp. 23–28.

[29] L. Hadjidemetriou, E. Kyriakides, Y. Yang, and F. Blaabjerg, "A synchronization method for single-phase grid-tied inverters," *IEEE Transactions on Power Electronics*, vol. 31, no. 3, pp. 2139–2149, March 2016.

[30] S. B. Kjaer, J. K. Pedersen, and F. Blaabjerg, "A review of single-phase grid-connected inverters for photovoltaic modules," *IEEE Transactions on Industry Applications*, vol. 41, no. 5, pp. 1292–1306, Sept 2005.

[31] STMicroelectronics. Datasheet- stmicroelectronics. [Online]. Available: http://www.st.com/resource/en/datasheet/stpm34.pdf

List of Publications

- An IEEE conference paper on “A Technical Review in Solar-net metering” by Harjeet Singh Bedi, Nirbhowjap Singh and Mukesh Singh was presented at 7^{th} international IEEE conference IICPE-2016 at Thapar University, Patiala.
- An IEEE paper on “ A Novel Approach for Bi-directional Energy Metering Based on Integrated Rooftop SPV Systems” by Harjeet Singh Bedi, Mukesh Singh and Nirbhowjap Singh manuscript under preparation.

Curriculum Vitae of the Author

I. Introduction

Name	**:**	Harjeet Singh Bedi
Father's name	**:**	Mr. Harnam Singh Bedi
Date of birth	**:**	09/04/1994
e-mail	**:**	harjit.singh277@gmail.com

II. Educational Qualification

Examination	**Institute**	**Board/University**	**Marks(%)**
10^{th}	Modern Senior Secondary School, Patiala	Punjab School Education Board	79.60
12^{th}	DAV Public School, Patiala	Central Board of Secondary Education	66.00
B.Tech.(EE)	SUS, Tangori, Mohali	PTU, Jalandhar	72.75
M.E.(Power Systems)*	Thapar University, Patiala	Thapar University	7.76 (CGPA)

* Till third semester.